



Published in final edited form as:

J Med Chem. 2010 October 28; 53(20): 7414–7427. doi:10.1021/jm100884b.

Discovery of novel 2-aryl-4-benzoyl-imidazoles targeting the colchicines binding site in tubulin as potential anticancer agents

Jianjun Chen^a, Zhao Wang^a, Chien-Ming Li^{b,c}, Yan Lu^a, Pavan K. Vaddady^a, Bernd Meibohm^a, James T. Dalton^{b,c}, Duane D. Miller^{a,c}, and Wei Li^{a,*}

^a Department of Pharmaceutical Sciences, University of Tennessee Health Science Center, Memphis, TN 38163

^b Division of Pharmaceutics, College of Pharmacy, The Ohio State University, Columbus, OH, 43210

^c GTx, Inc., Memphis, TN 38163

Abstract

A series of 2-aryl-4-benzoyl-imidazoles (ABI) was synthesized as a result of structural modifications based on the previous set of 2-aryl-imidazole-4-carboxylic amide (AICA) derivatives and 4-substituted methoxybenzoyl-aryl-thiazoles (SMART). The average IC₅₀ of the most active compound (**5da**) was 15.7 nM. ABI analogs have substantially improved aqueous solubility (48.9 µg/mL for **5ga** vs. 0.909 µg/mL for **SMART-1**, 0.137 µg/mL for paclitaxel, and 1.04 µg/mL for Combretastatin A4). Mechanism of action studies indicate that the anticancer activity of ABI analogs is through inhibition of tubulin polymerization by interacting with the colchicine binding site. Unlike paclitaxel and colchicine, the ABI compounds were equally potent against multidrug resistant cancer cells and the sensitive parental melanoma cancer cells. In vivo results indicated that **5cb** was more effective than DTIC in inhibiting melanoma xenograph tumor growth. Our results suggest that the novel ABI compounds may be developed to effectively treat drug-resistant tumors.

Keywords

imidazole; ABI; SMART; melanoma; prostate cancer; antiproliferative activity; structure-activity relationship; tubulin polymerization inhibitor

Introduction

Cancer is one of the main causes of death ranked only after heart disease. While existing therapies are effective in treating various cancers in their early stages, efficacy against metastatic cancers is far from satisfactory. With the rapid increasing of cancers in the U.S. and worldwide, clearly, there is an urgent need to develop highly effective anticancer drugs, which is the goal of our research. We previously described 2-aryl-imidazole-4-carboxylic amide (AICA) derivatives (Figure 1) as potent antiproliferative agents for melanoma.¹ The most potent compounds in the AICA series have average IC₅₀ values ranging from 3.5 to 10 µM on melanoma cells.¹ More recently, we reported a series of novel substituted

*To whom correspondence should be addressed. Telephone: (901)448-7532. Fax: (901)448-6828. wli@uthsc.edu.

Supporting Information Available: Dose response curves in Pgp-mediated multidrug resistant and their parental sensitive melanoma cell lines for compounds **5cb**, **4cb** and **4fb**; competitive binding at the colchicine site in tubulin for compound **5cb**; analytical and spectroscopic data for all final compounds. This materials is available free of charge via the Internet at <http://pubs.acs.org>.

methoxybenzoyl-aryl-thiazole (SMART) compounds that possess nanomolar activity in inhibiting melanoma and prostate cancer cell growth *in vitro*.² Preliminary studies showed that the SMART compounds disrupt tubulin polymerization, and therefore effectively prevent the formation of functional microtubules and block cell mitosis.² SMART compounds also showed great promise in overcoming P-glycoprotein (Pgp) mediated MDR *in vitro*.³ Despite the high activity, most SMART compounds are hydrophobic and have limited water solubility, which requires extensive use of surfactants to solubilize a sufficient amount of drug for effective dosing or the use of advanced drug delivery strategies.³ In addition, it has been reported that the thiazole ring, which is present in the SMART compounds, may undergo oxidative cleavage resulting in a nitroxide and ultimately in reduced *in vivo* stability for SMART compounds.⁴

We hypothesized that replacing the thiazole ring of the SMART compounds with an imidazole to give aryl-benzoyl-imidazoles (ABI) would be highly beneficial for the following reasons. First, the imidazole moiety is present in many existing drugs and has been proven to be very stable.⁵ Second, compared with the thiazole ring, the imidazole ring is much more hydrophilic, is expected to have improved aqueous solubility, and thus may simplify formulation and *in vivo* use. Finally, the imidazole is slightly acidic under physiological conditions. It is well known that the microenvironment inside a tumor is slightly acidic because of a higher production of lactic acid from glycolysis (the Warburg effect).⁶ The ABI analogs should exist predominantly in the unionized state under these conditions. As a result, ABI analogs may more easily pass through the cancer cell membrane and conceivably achieve higher intratumoral drug concentrations and greater *in vivo* potency.

In this paper, we describe our efforts to synthesize a focused set of ABI analogs (Figure 1), to understand their structure-activity relationships, to assess their efficacy *in vivo*, and to further elucidate their mechanism of action. The ABI analogs consist of three conjugated aromatic rings (denoted as rings A, B, and C in Figure 1). An imidazole ring was introduced as the B ring in the ABI series to replace the thiazole ring in the SMART series. The linker between the B and C rings was modified from an amide in the AICA derivatives to a carbonyl group in ABIs. For the C ring, different substituted phenyls were introduced. We show that replacing the thiazole ring with an imidazole ring retained the antiproliferative activity with significantly improved water solubility. Mechanism of action studies indicated that the ABI analogs work by competitively binding to the colchicine binding site in the α/β tubulin dimer and disrupting tubulin polymerization. However, unlike existing drugs targeting tubulin such as paclitaxel and vinblastine, the ABI compounds are equally effective against multidrug-resistant cancer cells; therefore, they hold great promise as potential drugs to treat resistant cancer.

Chemistry

The general synthesis of the ABI analogs is outlined in Schemes 1–3. First, a series of imidazolines (**7b-x**) was synthesized by reacting the appropriately substituted benzaldehyde with ethylene diamine in the presence of iodine and potassium carbonate (Scheme 1).⁷ Second, the imidazoline (**7b-x**) was oxidized to the corresponding imidazole catalyzed by diacetoxyiodobenzene.⁷ Compounds **2b** and **2x** were generated by this method. However, it was not successful when applied to other analogs with different substitutions in the A ring. Consequently, bromotrichloromethane and DBU were used as the oxidizing agents to convert imidazoline to the corresponding imidazole.⁸ Although compound **2c** was produced by this means, this method was discontinued because of poor yield (<5%). Other attempts were also made by using different oxidizing agents including the activated carbon-O₂ system⁹ and palladium-carbon system,¹⁰ but neither of these methods gave a satisfactory

yield (<2%). In our efforts to find an alternative way to construct the imidazole ring, we tried starting with iminoether¹¹ but abandoned this approach because of the multistep synthesis. Finally, a simple, one-step synthesis of the key intermediate (**2a-k**) was found (Scheme 2) by reacting the appropriate benzaldehyde (**1a-h**) in ethanol with oxalaldehyde and ammonia hydroxide to construct the imidazole ring system (**2a-k**).¹² The yield from this method was not high (approximately 20–40%), but it was acceptable to conduct the subsequent reactions. 2-Aryl-1*H*-imidazole (**2a-k**) was then converted to the *N*-phenylsulfonyl protected 2-aryl-imidazoles (**3a-k**) by treating with phenylsulfonyl chloride and sodium hydride in THF.¹³ Compounds **3a-k** were coupled with an appropriately substituted benzoyl chloride in the presence of tert-butyl lithium to obtain the aryl (2-aryl-1-(phenylsulfonyl)-1*H*-imidazol-4-yl) methanone (**4ab-jb**).¹³ Removing the protecting group from **4ab-jb** by tetrabutylammonium fluoride in THF gave the desired ABI agents (**5aa-hb**).¹³ Compounds **5aba** and **5aaa** were straightforwardly prepared based on the reaction of 2-phenyl-1*H*-imidazole (**2a**) with an appropriate benzoyl chloride following a known method (Scheme 3).¹⁴ Compounds **6ea**, **6fa**, and **6ha** were afforded by treating **5ea**, **5fa**, **5ha**, respectively, with BBr₃ to remove the methyl groups. Likewise, debenzoylation of **5ja** and **5jb** by concentrated HCl provided **5ka** and **5kb**, respectively.

Biological Results and Discussion

We first assessed the *in vitro* antiproliferative activities of these compounds using three melanoma cell lines (one murine melanoma cell line, B16-F1, and two human metastatic melanoma cell lines, A375 and WM-164) and four human prostate cancer cell lines (LNCaP, PC-3, Du 145, and PPC-1). The results are summarized in Tables 1–4.

Effects of substitutions on the C ring (Table 1)

A variety of compounds (**5aa-5ai**) with an unsubstituted A-ring and different C-ring substituents generally showed moderate activity (Table 1), with IC₅₀ values in the μM range (unless specified, the IC₅₀ value for a specific compound discussed in the text is referred to as an average of all seven cell lines). The most potent compound of this series was **5aa** with an average IC₅₀ value of 160 nM. The removal of one of the methoxy groups from the 3, 4, 5-trimethoxy on the C ring (**5ad**, **5ae**) led to a significant loss of activity (IC₅₀ >10 μM for **5ae** and an IC₅₀ of 3.1 μM for **5ad**). This finding is consistent with results from SMART compounds in which the 3, 4, 5-trimethoxy substituted compound was most potent. It should be noted that the compound with 4-fluoro on the C ring (**5af**) also showed relatively good activity (IC₅₀ = 0.91 μM), a finding that has an important implication, because replacing the trimethoxy moiety with a 4-fluoro group may provide good activity and improved metabolic stability. Interestingly, the position of the fluorine on the C ring was critical for activity because a shift from 4-fluoro to 3-fluoro resulted in a total loss of activity (IC₅₀ >10 μM for **5ag** compared with 0.91 μM for **5af**). This result suggested that a potential hydrogen bond donor is present close to the 4-position of this ring. As shown in the molecular modeling studies below, this hydrogen bond donor is likely to be the thiol group in Cys-241 in loop 7 of the β-subunit in α/β-tubulin dimer. Other substituents such as methoxy and methyl at the 3 or 4 position on the C ring (**5ab**, **5ac**, **5ah**, **5ai**) were also evaluated, but none showed good activity (IC₅₀ > 10 μM). As clearly indicated in Table 1, the positions of the A and C rings were critical. A simple shift of the C-ring moiety from position 4 to position 1 in the imidazole ring (B ring) resulted in total loss of activity (IC₅₀ >10 μM for **5aba**, **5aaa**, **3a**, **3x**, **3j**). This result is consistent with recent reports in which the position of the aryl group was found to be important for antiproliferative activity.^{15, 16} Bellina and co-workers reported potent antitumor activity for a series of 1, 5- and 1, 2-diaryl-1*H*-imidazole analogs. While the 1, 5-diaryl-imidazole analogs have nanomolar activity, a simple shift of the diaryl substitution from the 1, 5-position to 1, 2-position resulted in significantly lower activity

down to the micromolar range.¹⁵ Similarly, Wang and co-workers reported that 4, 5-disubstituted and 1, 5-disubstituted imidazoles are much more active than the corresponding 1, 2-disubstituted imidazoles.¹⁶

Effects of substitutions on the A ring (Table 2)

Because compounds with 3, 4, 5-trimethoxy and 4-fluoro substitutions on the C ring showed good activity, a series of compounds was synthesized with fixed substitutions on the C ring (4-fluoro or 3, 4, 5-trimethoxy) and different substitutions on the A ring (Table 2). These compounds demonstrated excellent antiproliferative activity with IC₅₀ values as low as 8.0 nM on WM164 cell line (**5da**). In general, compounds incorporating a single substituent on the para-position of the A ring were more potent as can be seen from the activities of **5ca**, **5cb**, **5da**, **5db**, **5fa**, **5fb**, **5ga**, and **5gb** (IC₅₀ = 7.9–110 nM). **5db**-HCl salt (IC₅₀ = 172 nM) showed slightly diminished activity compared with the corresponding free base **5db** (IC₅₀ = 109 nM). Compound **5fb** (IC₅₀ = 63.7 nM) which has a single halogen substituent in the para-position of the A and C rings, demonstrated potency and was devoid of a methoxy moiety. Compounds with 3, 4, 5-trimethoxy substituents on the A ring lost activity completely (IC₅₀ > 10 μM for **5ea**, **5eb**), suggesting very different binding environments near the A ring and C ring. Removal of the 5-methoxy substituent from the A-ring improved activity significantly (IC₅₀ = 330 nM and >10 μM for **5ha**, **5ea** respectively). Demethylation of the 3, 4, 5-trimethoxy decreased activity sharply from 43 nM (**5fa**) to 3.89 μM (**6fa**). Similar results were observed for **6ea**, **5ka**, **5kb**, and **6ha** due to the demethylation of substituents on either the A or C ring. Electron-donating groups (4-methoxy, 4-dimethylamino, 4-methyl) and electron-withdrawing groups (4-chloro, 4-trifluoromethyl) on the A ring did not show substantial differences in activity. The introduction of a trifluoromethyl group at the para-position of the A ring (IC₅₀ = 193 nM for **5la**) led to a 12-fold decrease of activity compared with compound **5da** (IC₅₀ = 15.7 nM) which has a methyl group at the para-position. In addition, a shift of the trifluoromethyl group from para to ortho position in the A ring caused complete loss of activity (IC₅₀ >10 μM for **5ia**, **5ib**), consistent with the results with other substituents. The presence of a benzoxo group at the para position of A ring (IC₅₀ = 75 nM for **5jb**) resulted in a 440-fold increase in activity when compared with the para-hydroxy compound **5kb** (IC₅₀=33 μM). It is worthwhile to note that compound **5jb**, with the 4-fluoro in the C ring, has better activity than does its counterpart **5ja**, which has a 3, 4, 5-trimethoxy group in the C ring (IC₅₀ is 75 nM for **5jb**, and 7.3 μM for **5ja**).

Effects of additional substitutions on the B ring (Table 3)

Interestingly, some of the compounds with a phenylsulfonyl protection group attached to the nitrogen of the imidazole ring (**4cb**, **4db**, **4fb**, **4ga**, **4gb**, **4ha**, **4jb**) were also very active with IC₅₀ in the nM range (Table 3). Generally the activities of these compounds are comparable to their corresponding unprotected counterparts as exemplified by comparing the activities of **4cb** (43 nM), **4db** (111 nM), **4fb** (72 nM), **4ga** (285 nM), **4gb** (87 nM), **4ha** (268 nM), and **4jb** (61 nM) with their corresponding unprotected counterparts **5cb** (36 nM), **5db** (109 nM), **5fb** (64 nM), **5ga** (131 nM), **5gb** (72 nM), **5ha** (330 nM), and **5jb** (75 nM). Other compounds (**4ab**-**4ag**, **4ea**, **4eb**, **4hb**, **4ia**, and **4ib**, 1–50 μM) were generally much less active, also in line with their counterparts (**5ab**-**5ag**, **5ea**, **5eb**, **5hb**, **5ia**, and **5ib**, 1–50 μM). The comparable activity of these N-protected compounds with their unprotected counterparts may suggest that they may have similar binding interactions to their target. It is possible that the N-protection group does not contribute significantly to the binding for these compounds, as we will see from the molecular modeling studies for compounds **4cb** and **5cb**.

ABI compounds are effective against multidrug resistant melanoma cells (Table 4)

Pgp-mediated drug efflux represents a major mechanism for cancer cells to prevent the build up of effective anticancer intracellular drug concentrations. We compared the activity of the ABI compounds against multidrug resistant melanoma cells (MDA-MB-435/LCCMDR1) and their parental nonresistant cancer cells (MDA-MB-435). Although MDA-MB-435 was originally designated as a breast cancer cell line, it has been shown definitively to originate from the M14 melanoma cell line.^{17–19} This pair of cell lines have been well validated and widely used to assess abilities of drugs overcoming Pgp-mediated MDR.^{20–23} Compounds **5cb**, **4cb**, and **4fb** together with other tubulin-targeting agents including colchicine, paclitaxel, and vinblastine were tested on both the MDR melanoma cell line and its parental melanoma cell line (Table 4). Compounds **5cb**, **4cb**, **4fb** had much better resistance indices (1.3 for **5cb**, 0.8 for **4cb**, 0.7 for **4fb**) than colchicine (65.8), paclitaxel (69.3), and vinblastine (27.5). Although colchicine, paclitaxel, and vinblastine showed excellent activity in nonresistant melanoma cell lines (0.5–10 nM), these compounds were significantly less potent in the MDR melanoma cell line (277–658 nM). In contrast, **5cb**, **4cb**, **4fb** had essentially equivalent potency on both MDR (30 nM, 30 nM, 35 nM for **5cb**, **4cb** and **4fb** respectively) and nonresistant melanoma cellines (24 nM, 38 nM, 50 nM for **5cb**, **4cb** and **4fb** respectively).

ABI compound 5cb is highly active in vivo

To evaluate efficacy of ABI analogs in vivo, we tested the antitumor activity of compound **5cb** on mice melanoma B16-F1 xenograph. DTIC, the gold standard in malignant melanoma treatment, was used as a positive control.²⁴ Compound **5cb** was selected for the in vivo studies because it is more stable compared with compound **5da**, although **5da** (IC₅₀=15.7 nM) showed higher in vitro potency than **5cb** (IC₅₀=35 nM), it has been proven to be susceptible to demethylation due to the presence of the 3, 4, 5-trimethoxy moiety on the C-ring.²⁵ Twenty female C57/BL mice were divided into four groups: a vehicle control group, a DTIC (60 mg/kg) treatment group,²⁴ a **5cb** (10 mg/kg) treatment group, and a **5cb** (30 mg/kg) treatment group. Each mouse was injected with 0.5 million B16-F1 melanoma cells subcutaneously. Seven days after tumor inoculation, treatment started with each compound injected intraperitoneally daily (Figure 2). Tumor volume was significantly ($p < 0.05$) reduced 47%, 51%, and 73% for **5cb** (10 mg/kg), DTIC (60 mg/kg), and **5cb** (30 mg/kg), respectively, after 14 days of treatment. No significant weight loss was observed in any of the treatment groups during the experiment.

ABI analogs have significantly higher water solubility than SMART analogs (Table 5)

We compared the HPLC retention times of ABI compound **5ga** (1.5 min) and its corresponding SMART analog (**SMART-1**, 2.2 min) using 80/20 methanol/water mobile phase at 1 mL/min flow rate and a reversed phase column, indicating that the imidazole derivative was more hydrophilic than its corresponding SMART analog. The calculated logP values for ABI compound **5ga** and the corresponding SMART analog (**SMART-1**) were approximately 2.9 and 4.4, respectively. We also determined the aqueous solubility of compound **5ga** and its corresponding SMART analog (**SMART-1**) using a minituarized shake-flask method and LC-MS/MS quantification. The aqueous solubility of compound **5ga** was 48.9 µg/mL and 11.3 µg/mL in buffer pH7.0 and water, respectively, or about 50 and 10 times greater than its SMART counterpart, **SMART-1** (0.909 µg/mL and 0.83 µg/mL in buffer pH7.0 and water, respectively). Combrestastatin A4 (CA-4) and paclitaxel were used as positive controls because of their well-established anti-tumor activity and extensive

studies on these two compounds. It is also very interesting to compare the aqueous solubility of ABI analogs with CA-4 and paclitaxel since they all target tubulin polymerization (see below for mechanism studies for ABI analogs). The aqueous solubility determined in this parallel experiment was 1.04 $\mu\text{g/mL}$ in buffer pH7.0 and 2.83 $\mu\text{g/mL}$ in water for CA-4, and 0.137 $\mu\text{g/mL}$ in buffer pH7.0 and 0.021 $\mu\text{g/mL}$ in water for paclitaxel. Collectively, these results indicate that **5ga** and presumably other ABI analogs, due to the high structural similarity with **5ga**, have much higher aqueous solubility than their SMART counterparts.

Mechanism of action studies

We hypothesized that the ABI compounds have a similar mechanism of action to the SMART compounds that involve binding to the colchicine site in tubulin α/β -heterodimer. We first performed experiments to confirm the inhibition of tubulin polymerization by ABI compounds. Bovine brain tubulin (>97% pure) was incubated with three potent ABI compounds, **5cb**, **5da**, and **5db** at a concentration of 10 μM , to determine the effect of these ABI compounds on tubulin polymerization (Figure 3A). Tubulin polymerization was completely inhibited by compound **5da**, while ~80% inhibition was observed during incubation with compounds **5cb** and **5db**.

Three ligand binding sites in tubulin α/β -heterodimer have been reported: paclitaxel binding site,²⁶ vinblastine binding site,^{26, 27} and colchicine binding site.^{26–28} The structural similarity with the SMART compounds and the effects on tubulin polymerization prompted us to hypothesize that ABI compounds bind to the colchicine binding site in tubulin. We measured the binding affinity of compound **5cb** using ³H-labeled colchicine and a competitive binding scintillation proximity assay (SPA).²⁹ The results confirmed the strong binding of **5cb** with a binding affinity of $3.4 \pm 1.5 \mu\text{M}$ (Figure 3B). Colchicine bound tubulin with an IC_{50} value of $1.8 \pm 0.5 \mu\text{M}$ under these conditions. These results clearly indicated that ABI compounds effectively inhibit tubulin polymerization, similar to the protocol SMART compounds.

Proposed binding mode of ABI binding at the colchicine binding site

We next investigated with molecular modeling the possible binding mode for these compounds in tubulin. Several crystal structures of the ligand-tubulin complex are available in the PDB databank,^{27, 28, 30} with the most recent one from Dorleans et al.³⁰ In general, the colchicine binding pocket tolerates a variety of molecular structures, which may indicate substantial conformation changes upon ligand binding. In fact, Dorleans et al. solved the crystal structures of both the empty tubulin dimer and the ligand-tubulin complex.³⁰ They found that, without the presence of ligand, loop 7 (T7, residues 244–251, Figure 4) in the beta-monomer folds in to occupy the binding pocket, while it flips out upon ligand binding. The associated helix 7 (H7, residues 224–243) and helix 8 (H8, residues 252–260) were displaced upon ligand binding. It is conceivable that the extent to which T7 is displaced depends on the size of individual ligand. This flexibility presents a significant challenge to understand the precise binding modes for individual ligands without solving actual crystal structures. Nevertheless, careful analysis of the possible binding modes could provide some insights into the binding of different ligands.

The binding modes of **5cb** and **4cb** (stick model) are shown in Figure 4A and 4B. For comparison, we also displayed the crystal structure complexes of ABT-751 and DAMA-colchicine (wire models) along with ABI-**5cb**/tubulin complex in Figure 4A. For clarity, only the related secondary structures forming the binding pocket in β -tubulin are shown in Figure 4A. The overall structures of **5cb**, ABT-751 and DAMA-colchicine overlapped very well in the binding pocket. Several potential hydrogen bonding interactions between compound **5cb** and tubulin were identified. The carbonyl group in **5cb** was in sufficient

proximity to form two hydrogen bond interactions with the backbone NH of Leu-252 in H8 and the sidechain of Asp-251 in T7 of the tubulin β -monomer. The para-fluorine substituent in the C-ring was close to the sidechain of Cys241 in T7 and Tyr202 in S6, possibly forming one or two hydrogen bonds. The imidazole proton is very close and likely to form a hydrogen bond to Thr179 in T5 loop (residues 173–182) of the tubulin α -monomer (Figure 4A). Many of these interactions are consistent with literature reports with closely related ligands. Together with the hydrophobic interactions provided by the aromatic rings, the likely formation of these hydrogen bonds would contribute to the high binding affinity to the tubulin dimer, resulting in high antiproliferative potency.

The binding mode of **4cb** will be conceivably less defined since two of the three aromatic rings may occupy the binding pocket in the β -monomer while the third ring may extend toward the interface of the α/β -monomers, similar to how the sidechain of DAMA-chochicine binds. Our modeling indicates that the protecting group likely extends to the tubulin dimer interface, while the A, C rings of **4cb** occupy similar binding pocket and orientation as **5cb** (Figure 4B). This may explain the similar activity between the two compounds, even though **4cb** has an extra ring system. If this is true, it is possible to design new generations of ligands by properly incorporating more hydrophilic groups to further improve aqueous solubility.

Conclusions

We synthesized a set of novel 2-aryl-4-benzoyl-imidazole (ABI) derivatives that showed potent activity in a number of cancer cell lines, as well as in a xenograft model. The compounds inhibited tubulin polymerization by binding to the colchicine binding site. Structure activity relationships (SAR) (Figure 5) were investigated by introducing different substituents into the A and C rings. Compared with the earlier SMART compounds and other well-established anticancer agents such as paclitaxel and DTIC, ABI analogs showed three improvements. First, aqueous solubility was significantly improved (**5ga**, 48.9 $\mu\text{g/mL}$) compared with SMART analogs (**SMART-1**, 0.909 $\mu\text{g/mL}$). Compared with CA-4, which has a similar mechanism of action, **5ga** has at least 15-fold higher aqueous solubility. This is an important improvement, because one general problem with drugs targeting tubulin polymerization such as paclitaxel is the poor aqueous solubility. In fact, in the ongoing clinical trial with CA-4, due to its poor aqueous solubility, its phosphate pro-drug (CA-4P) has to be used.³¹ Second, compound **5cb** showed a much better resistance index (1.3) compared with colchicine (65.8), paclitaxel (69.3), and vinblastine (27.5). The fact that **5cb** can overcome multidrug resistance suggests a promising future development of more drug-like agents. Third, our *in vivo* study showed that compound **5cb** at a dose of 30mg/kg gave better tumor suppression than that of DTIC at a dose of 60mg/kg. Additional work is underway to test these compounds in other types of cancers to further optimize their efficacy.

Experimental Section

General

All reagents were purchased from Sigma-Aldrich Chemical Co., Fisher Scientific (Pittsburgh, PA), Alfa Aesar (Ward Hill, MA), and AK Scientific (Mountain View, CA) and were used without further purification. The solvents for moisture-sensitive reactions were freshly distilled, and the reactions were carried out under an argon atmosphere. Routine thin layer chromatography (TLC) was performed on aluminum-backed Uniplates (Analtech, Newark, DE). Melting points were measured with Fisher-Johns melting point apparatus (uncorrected). NMR spectra were obtained on a Varian Inova-500 spectrometer or a Bruker AX 300 (Billerica, MA) spectrometer. Chemical shifts are reported as parts per million

(ppm) relative to TMS in CDCl₃. Mass spectra were collected on a Bruker ESQUIRE electrospray/ion trap instrument in positive and negative ion modes. The purity of the final compounds was tested via RP-HPLC on a Waters 2695 HPLC system installed with a Photodiode Array Detector. Two RP-HPLC methods were conducted using a Supelco Ascentis™ 5μM C-18 column (250 × 4.6 mm) at ambient temperature, and a flow rate of 0.7 mL/min. HPLC1: Gradient: Solvent A (water) and Solvent B (methanol): 0–20 min 40–100%B (linear gradient), 20–27 min 100%B. HPLC2: Gradient: Solvent A (water) and Solvent B (methanol): 0–15 min 40–100%B (linear gradient), 15–25 min 100%B. UV detection at 254nm. Purities of the compounds were established by careful integration of areas for all peaks detected and are reported for each compound in the following section.

General procedure for the preparation of 2-aryl-1*H*-imidazole (2a-l, x)

Method A (essential for only **2b**, **2x**): To a solution of 2-aryl-4, 5-dihydro-1*H*-imidazole **7** (35 mmol) in DMSO (100 ml) was added potassium carbonate (38.5 mmol) and diacetoxyiodobenzene (38.5 mmol). The reaction mixture was stirred overnight in darkness. Water was added followed by extraction with dichloromethane. The organic layer was dried over magnesium sulfate and concentrated. The residue was subjected to flash column chromatography (hexane: ethyl acetate 3:2) to give a white solid. Yield: 30%-50%. This method worked for only **2b** and **2x**, but not for the other compounds for unknown reasons. Method B (essential for only **2c**): To a solution of 2-aryl-4, 5-dihydro-1*H*-imidazole **7** (50 mmol) in DMF (70 ml) was added DBU (55 mmol) and CBrCl₃ (55 mmol). The reaction mixture was stirred overnight and a saturated NaHCO₃ (aqueous) solution was added followed by extraction with dichloromethane. The organic layer was dried over magnesium sulfate and concentrated. The residue was subjected to flash column chromatography (chloroform: methanol 50:1) to yield a white solid. Yield: 7%.

Method C (essential for **2a**, **2d-l**): To a solution of appropriate benzaldehyde **1** (100 mmol) in ethanol (350 ml) at 0°C was added a solution of 40% oxalaldehyde in water (12.8 ml, 110 mmol) and a solution of 29% ammonium hydroxide in water (1000 mmol, 140 ml). After stirring for 2–3 days at room temperature, the reaction mixture was concentrated and the residue was subjected to flash column chromatography with dichloromethane as eluent to yield the titled compound as a yellow powder. Yield: 20%–40%.

General procedure for the preparation of 2-aryl-1- (phenylsulfonyl)-1*H*-imidazole (3a-l, x)

To a solution of 2-aryl-1*H*-imidazole **2** (20 mmol) in anhydrous THF (200 ml) at 0°C was added sodium hydride (60% dispersion in mineral oil, 1.2 g, 30 mmol) and stirred for 30 min. Benzenesulfonyl chloride (2.82 ml, 22 mmol) was added and the reaction mixture was stirred overnight. After dilution by 100 ml of saturated NaHCO₃ solution (aqueous), the reaction mixture was extracted by ethyl acetate (500 ml). The organic layer was dried over magnesium sulfate and concentrated. The residue was purified by flash column chromatography (hexane: ethyl acetate 2:1) to give a pale solid. Yield: 40%–50%.

General procedure for the preparation of aryl (2-aryl-1- (phenylsulfonyl)-1*H*-imidazol-4-yl) methanone (4aa-ai, ba, ca, cb, da, db, ea, eb, fa, fb, ga, gb, ha, hb, ia, ib, ja, jb, la)

To a solution of 2-aryl-1- (phenylsulfonyl)-1*H*-imidazole (6.0 mmol) **3** in anhydrous THF (30 ml) at –78°C was added 1.7M tert-butyllithium in pentane (5.3 ml, 9.0 mmol) and stirred for 10 min. Appropriate substituted benzoyl chloride (7.2 mmol) was added at –78°C and stirred for overnight. The reaction mixture was diluted with 100 ml of saturated NaHCO₃ solution (aqueous) and extracted by ethyl acetate (200 ml). The organic layer was

dried over magnesium sulfate and concentrated. The residue was purified by flash column chromatography (hexane: ethyl acetate 4:1) to give a white solid. (Note: Due to the limited amount of starting material or the difficulty of separation, the following products formed in this step were used without further purification as a mixture for the next step: **4aa**, **4ad**, **4ae**, **4ai**, **4ba**, **4ca**, **4da**, **4fa**, **4ja**). Yield: 15%–40%.

General procedure for the preparation of aryl (2-aryl-1*H*-imidazol-4-yl) methanone (5aa-ai, ba, ca, cb, da, db, ea, eb, fa, fb, ga, gb, ha, hb, ia, ib, ja, jb, la)

To a solution of aryl (2-aryl-1-(phenylsulfonyl)-1*H*-imidazol-4-yl) methanone (2.0 mmol) **4** in THF (20.0 ml) was added 1.0M tetrabutyl ammonium fluoride (4.0 mmol) and stirred overnight. The reaction mixture was diluted by 50 ml of saturated NaHCO₃ solution (aqueous) and extracted by ethyl acetate (100 ml). The organic layer was dried over magnesium sulfate and concentrated. The residue was purified by flash column chromatography (hexane: ethyl acetate 3:1) or recrystallized from water and methanol to give a white solid. Yield: 80–95%.

General procedure for the preparation of (2-(4-hydroxyphenyl)-1*H*-imidazol-4-yl) (aryl) methanone (5ka, 5kb)

To a solution of (2-(4-(benzyloxy) phenyl)-1*H*-imidazol-4-yl)(aryl) methanone **5** (**5ja** or **5jb**, 1 mmol) in AcOH(20 ml) was added concentrated HCl (2 ml) and refluxed overnight. After removing the solvent, the residue was recrystallized from dichloromethane to give the titled compound as a yellow solid. Yield: 70–85%.

General procedure for the preparation of aryl (2-phenyl-1*H*-imidazol-1-yl) methanone (5aba, 5aaa)

To a solution of 2-phenyl-1*H*-imidazole **2a** (10 mmol) in THF (20 ml) was added NaH (15 mmol) and substituted benzoyl chloride (12 mmol) at 0°C. The reaction mixture was stirred overnight and diluted by saturated NaHCO₃ solution followed by extraction with ethyl acetate. The organic layer was dried over magnesium sulfate and concentrated. The residue was purified by flash column chromatography (chloroform) to give a white solid. Yield: 12–16%.

General procedure for the preparation of (2-aryl-1*H*-imidazol-4-yl) (3, 4, 5-trihydroxyphenyl) methanone **6 (6ea, 6fa, 6ha)**

To a solution of aryl (2-aryl-1*H*-imidazol-4-yl) methanone **5** (**5ea**, **5fa**, **5ha**). (0.5 mmol) in CH₂Cl₂ (6.0 ml) was added 1.0 M of BBr₃ (2 mmol) in CH₂Cl₂ and stirred for 1h at room temperature. Water was added to destroy excess BBr₃. The precipitated solid was filtered and recrystallized from MeOH to afford a yellow solid. Yield: 60–80%.

General procedure for the preparation of 2-aryl-4, 5-dihydro-1*H*-imidazole **7 (7b, 7c, 7x)**

To a solution of appropriate benzaldehyde **1** (60 mmol) in t-BuOH (300 ml) was added ethylenediamine (66 mmol) and stirred for 30 min at room temperature. Potassium carbonate (75 mmol) and iodine (180 mmol) were added to the reaction mixture sequentially followed by stirring at 70°C for 3 h. Sodium sulfite (Na₂SO₃) was added and the mixture was extracted by chloroform. The organic layer was dried over magnesium sulfate and concentrated. The residue was purified by flash column chromatography (chloroform: methanol 20:1) to give a white solid. Yield: 50–60%.

General procedure for the preparation of aryl (2-aryl-1*H*-imidazol-4-yl) methanone-HCl salt (5db-HCl)

To a solution of **5db** (0.5 mmol) in methanol (20 ml) was added 2M solution of hydrogen chloride (5 mmol) in ethyl ether and stirred overnight at room temperature. The reaction mixture was concentrated and the residue was washed by CH₂Cl₂ to yield the titled compound. Yield: 95%.

2-Phenyl-1*H*-imidazole (2a)

Yield: 36.8 %. ¹H NMR (500MHz, DMSO) δ 12.52 (br, 1H), 7.95 (d, *J* = 7.0 Hz, 2H), 7.44 (t, *J* = 7.5 Hz, 2H), 7.34 (t, *J* = 7.0 Hz, 1H), 7.25–7.27 (m, 1H), 7.04 – 7.07 (m, 1H). MS (ESI): calculated for C₉H₈N₂, 144.1, found 167.1 [M + Na]⁺.

2-(4-Fluorophenyl)-1*H*-imidazole (2b)

Yield: 56.5 %. ¹H NMR (300MHz, DMSO) δ 12.46 (br, 1 H), 7.94–7.99 (m, 2 H), 7.24–7.30 (m, 2 H), 7.00–7.03 (m, 2 H). MS (ESI): calculated for C₉H₇FN₂, 162.1, found 163.0 [M + H]⁺, 160.6 [M – H][–].

2-(4-Methoxyphenyl)-1*H*-imidazole (2c)

Yield: 22.2 %. ¹H NMR (500MHz, CDCl₃) δ 7.80 (d, *J* = 10.0 Hz, 2 H), 7.15 (s, 2 H), 3.86 (s, 3 H). MS (ESI): calculated for C₁₀H₁₀N₂O, 174.1, found 175.0 [M + H]⁺, 172.8 [M – H][–].

2-(*p*-Tolyl)-1*H*-imidazole (2d)

Yield: 36.1 %. ¹H NMR (500MHz, CDCl₃) δ 7.64 (d, *J* = 7.5 Hz, 2 H), 7.16 (d, *J* = 7.5 Hz, 2 H), 7.12 (s, 1 H), 7.02 (s, 1 H). MS (ESI): calculated for C₁₀H₁₀N₂, 158.1, found 159.0 [M + H]⁺, 156.8 [M – H][–].

2-(3, 4, 5-Trimethoxyphenyl)-1*H*-imidazole (2e)

Yield: 26.0%. ¹H NMR (500MHz, CDCl₃) δ 7.26 (s, 2 H), 7.08 (d, *J* = 1.5 Hz, 2 H), 3.86 (s, 3 H), 3.82 (s, 6 H). MS (ESI): calculated for C₁₂H₁₄N₂O₃, 234.1, found 234.9 [M + H]⁺.

2-(4-Chlorophenyl)-1*H*-imidazole (2f)

Yield: 19.8 %. ¹H NMR (500MHz, DMSO) δ 13.60 (br, 1 H), 7.94 (d, *J* = 8.5 Hz, 2 H), 7.51 (d, *J* = 8.0 Hz, 2 H), 7.27 (s, 1 H), 7.03 (s, 1 H). MS (ESI): calculated for C₉H₇ClN₂, 178.0, found 178.9 [M + H]⁺.

4-(1*H*-Imidazol-2-yl)-N, N-dimethylaniline (2g)

Yield: 16.5 %. ¹H NMR (300MHz, CDCl₃) δ 7.70 (dd, *J* = 7.0 Hz, 2.0 Hz, 2 H), 7.10 (s, 2 H), 6.75 (dd, *J* = 9.0 Hz, 2.0 Hz, 2 H), 3.02 (s, 6 H). MS (ESI): calculated for C₁₁H₁₃N₃, 187.1, found 187.9 [M + H]⁺, 185.8 [M – H][–].

2-(3, 4-Dimethoxyphenyl)-1 *H*-imidazole (2h)

Yield: 22.0 %. ¹H NMR (500MHz, CDCl₃) δ 7.52 (d, *J* = 1.5 Hz, 1 H), 7.27–7.28 (m, 1 H), 7.14 (s, 2 H), 6.88 (d, *J* = 8.0 Hz, 1 H), 3.91 (s, 3 H), 3.87 (s, 3 H). MS (ESI): calculated for C₁₁H₁₂N₂O₂, 204.1, found 205.1 [M + H]⁺, 202.8 [M – H][–].

2-(2-(Trifluoromethyl)phenyl)-1H-imidazole (2i)

Yield: 25.5 %. ¹H NMR (500MHz, DMSO) δ 12.31 (br, 1 H), 7.84 (d, *J* = 8.0 Hz, 1 H), 7.76 (t, *J* = 8.0 Hz, 1 H), 7.65 (t, *J* = 7.5 Hz, 1 H), 7.16 (br, 2 H). MS (ESI): calculated for C₁₀H₇F₃N₂, 212.1, found 212.9 [M + H]⁺, 210.7 [M - H]⁻.

2-(4-(Benzyloxy)phenyl)-1H-imidazole (2j)

Yield: 12.1 %. ¹H NMR (500MHz, CDCl₃) δ 7.77 (d, *J* = 8.5 Hz, 2 H), 7.36–7.47 (m, 5 H), 7.10–7.18 (m, 2 H), 7.06 (d, *J* = 9.0 Hz, 2 H), 5.13 (s, 2 H). MS (ESI): calculated for C₁₆H₁₄N₂O, 250.1, found 251.1 [M + H]⁺, 248.8 [M - H]⁻.

2-(4-(Trifluoromethyl)phenyl)-1H-imidazole (2l)

Yield: 26.2 %; ¹H NMR (CDCl₃, 500MHz) δ 8.03 (d, *J* = 8.0 Hz, 2 H), 7.66 (d, *J* = 8.0 Hz, 2 H), 7.25 (s, 2 H). MS (ESI) calcd for C₁₀H₇F₃N₂ 212.1, found 213.1 [M + H]⁺.

2-(4-Nitrophenyl)-1H-imidazole (2x)

Yield: 53.7 %. ¹H NMR (500MHz, DMSO) δ 12.97 (br, 1 H), 8.32 (d, *J* = 9.0 Hz, 2 H), 8.17 (d, *J* = 9.0 Hz, 2 H), 7.42 (s, 1 H), 7.17 (s, 1H). MS (ESI): calculated for C₉H₇N₃O₂, 189.1, found 189.9 [M + H]⁺, 187.8 [M - H]⁻.

2-Phenyl-1-(phenylsulfonyl)-1H-imidazole (3a)

Yield: 50.3 %. ¹H NMR (500MHz, CDCl₃) δ 7.64–7.67 (m, 1H), 7.56 (t, *J* = 9.0 Hz, 1H), 7.32–7.48 (m, 9H), 7.12–7.16 (m, 1H). MS (ESI): calculated for C₁₅H₁₂N₂O₂S, 284.1, found 307.1 [M + Na]⁺.

2-(4-Fluorophenyl)-1-(phenylsulfonyl)-1H-imidazole (3b)

Yield: 56.9 %. ¹H NMR (500MHz, CDCl₃) δ 7.66 (d, *J* = 2.0 Hz, 1 H), 7.58 (t, *J* = 10.0 Hz, 1 H), 7.36–7.42 (m, 6 H), 7.12 (d, *J* = 2.0 Hz, 1 H), 7.06 (t, *J* = 10.0 Hz, 2 H). MS (ESI): calculated for C₁₅H₁₁FN₂O₂S, 302.1, found 300.8 [M - H]⁻.

2-(4-Methoxyphenyl)-1-(phenylsulfonyl)-1H-imidazole (3c)

Yield: 40.9 %. ¹H NMR (500MHz, CDCl₃) δ 7.62 (d, *J* = 5.0 Hz, 1 H), 7.56 (tt, *J* = 15.0 Hz, 5.0 Hz, 1 H), 7.32–7.43 (m, 6 H), 7.10 (d, *J* = 5.0 Hz, 1 H), 6.88 (dt, *J* = 16.0 Hz, 6.0 Hz, 2 H), 3.87 (s, 3 H). MS (ESI): calculated for C₁₆H₁₄N₂O₃S, 314.1, found 337.1 [M + Na]⁺, 312.9 [M - H]⁻.

1-(Phenylsulfonyl)-2-(p-tolyl)-1H-imidazole (3d)

Yield: 46.6%. ¹H NMR (500MHz, CDCl₃) δ 7.63 (d, *J* = 1.0 Hz, 1 H), 7.55 (t, *J* = 8.0 Hz, 1 H), 7.42 (d, *J* = 8.0 Hz, 2 H), 7.35 (t, *J* = 7.5 Hz, 2 H), 7.27–7.29 (m, 2 H), 7.16 (d, *J* = 7.5 Hz, 2 H), 7.10 (s, 1 H), 2.41 (s, 3 H). MS (ESI): calculated for C₁₆H₁₄N₂O₂S, 298.1, found 321.1 [M + Na]⁺.

1-(Phenylsulfonyl)-2-(3, 4, 5-trimethoxyphenyl)-1H-imidazole (3e)

Yield: 55.7%. ¹H NMR (500MHz, CDCl₃) δ 7.68 (d, *J* = 1.5 Hz, 1 H), 7.55 (t, *J* = 7.0 Hz, 1 H), 7.42 (d, *J* = 7.5 Hz, 2 H), 7.35 (t, *J* = 8.5 Hz, 2 H), 7.11 (d, *J* = 1.5 Hz, 2 H), 6.60 (s, 1 H), 3.90 (s, 3 H), 3.79 (s, 6 H). MS (ESI): calculated for C₁₈H₁₈N₂O₅S, 374.1, found 397.1 [M + Na]⁺.

2-(4-Chlorophenyl)-1-(phenylsulfonyl)-1H-imidazole (3f)

Yield: 54.9%. $^1\text{H NMR}$ (500MHz, CDCl_3) δ 7.65 (d, $J = 2.0$ Hz, 1 H), 7.58 (t, $J = 7.5$ Hz, 1 H), 7.43 (d, $J = 8.5$ Hz, 2 H), 7.38 (t, $J = 8.0$ Hz, 2 H), 7.34–7.36 (m, 4 H), 7.12 (d, $J = 1.5$ Hz, 1 H). MS (ESI): calculated for $\text{C}_{15}\text{H}_{11}\text{ClN}_2\text{O}_2\text{S}$, 318.0, found 341.0 $[\text{M} + \text{Na}]^+$.

N, N-Dimethyl-4-(1-(phenylsulfonyl)-1H-imidazol-2-yl) aniline (3g)

Yield: 48.3%. $^1\text{H NMR}$ (300MHz, CDCl_3) δ 7.59 (d, $J = 2.0$ Hz, 1 H), 7.55 (t, $J = 8.0$ Hz, 1 H), 7.45 (d, $J = 7.5$ Hz, 2 H), 7.28–7.38 (m, 4 H), 7.07 (d, $J = 2.0$ Hz, 1 H), 6.68 (d, $J = 8.5$ Hz, 2 H), 3.04 (s, 3 H). MS (ESI): calculated for $\text{C}_{17}\text{H}_{17}\text{N}_3\text{O}_2\text{S}$, 327.1, found 350.0 $[\text{M} + \text{Na}]^+$, 325.9 $[\text{M} - \text{H}]^-$.

2-(3, 4-Dimethoxyphenyl)-1-(phenylsulfonyl)-1H-imidazole (3h)

Yield: 60.3%. $^1\text{H NMR}$ (500MHz, CDCl_3) δ 7.64 (d, $J = 7.0$ Hz, 1 H), 7.55 (t, $J = 7.5$ Hz, 1 H), 7.40 (dd, $J = 8.5$ Hz, 1.5 Hz, 2 H), 7.35 (t, $J = 8.0$ Hz, 2H), 7.09 (d, $J = 2.0$ Hz, 1 H), 7.02 (dd, $J = 8.0$ Hz, 2.0 Hz, 1 H), 6.89 (d, $J = 1.5$ Hz, 1 H), 6.86 (d, $J = 8.0$ Hz, 1 H), 3.95 (s, 3 H), 3.81 (s, 3 H). MS (ESI): calculated for $\text{C}_{17}\text{H}_{16}\text{N}_2\text{O}_4\text{S}$, 344.1, found 367.0 $[\text{M} + \text{Na}]^+$.

1-(Phenylsulfonyl)-2-(2-(trifluoromethyl) phenyl)-1H-imidazole (3i)

Yield: 58.6%. $^1\text{H NMR}$ (500MHz, CDCl_3) δ 7.64–7.67 (m, 2 H), 7.61–7.63 (m, 3 H), 7.40–7.46 (m, 5 H), 7.16 (d, $J = 1.5$ Hz, 1 H). MS (ESI): calculated for $\text{C}_{16}\text{H}_{11}\text{F}_3\text{N}_2\text{O}_2\text{S}$, 352.1, found 353.1 $[\text{M} + \text{H}]^+$.

2-(4-(Benzyloxy)phenyl)-1-(phenylsulfonyl)-1H-imidazole (3j)

Yield: 62.0%; mp 102 – 104 °C. $^1\text{H NMR}$ (500MHz, CDCl_3) δ 7.56 (d, $J = 1.0$ Hz, 1 H), 7.46 (t, $J = 8.0$ Hz, 1 H), 7.20–7.40 (m, 11 H), 7.03 (d, $J = 1.0$ Hz, 1H), 6.89 (t, $J = 8.0$ Hz, 2 H), 5.08 (s, 2 H). MS (ESI): calculated for $\text{C}_{22}\text{H}_{18}\text{N}_2\text{O}_3\text{S}$, 390.1, found 413.1 $[\text{M} + \text{Na}]^+$. HPLC2: t_R 18.22 min, purity 95.9%.

1-(Phenylsulfonyl)-2-(4-(trifluoromethyl)phenyl)-1H-imidazole (3l)

Yield: 36.7 %; $^1\text{H NMR}$ (CDCl_3 , 500MHz) δ 7.75 (d, $J = 2.0$ Hz, 1 H), 7.69 (d, $J = 8.0$ Hz, 2 H), 7.65 (t, $J = 8.0$ Hz, 1 H), 7.60 (d, $J = 8.0$ Hz, 2 H), 7.48 (d, $J = 7.5$ Hz, 2 H), 7.43 (t, $J = 8.0$ Hz, 2 H), 7.22 (d, $J = 2.0$ Hz, 1 H). MS (ESI) calcd for $\text{C}_{16}\text{H}_{11}\text{F}_3\text{N}_2\text{O}_2\text{S}$ 352.1, found 553.1 $[\text{M} + \text{H}]^+$.

2-(4-Nitrophenyl)-1-(phenylsulfonyl)-1H-imidazole (3x)

Yield: 50%; mp 145 – 147 °C. $^1\text{H NMR}$ (500MHz, DMSO) δ 8.28 (d, $J = 8.5$ Hz, 2 H), 8.03 (d, $J = 1.5$ Hz, 1 H), 7.78 (t, $J = 7.5$ Hz, 1 H), 7.64–7.68 (m, 4H), 7.60 (t, $J = 8.0$ Hz, 2 H), 7.30 (d, $J = 1.5$ Hz, 1 H). MS (ESI): calculated for $\text{C}_{15}\text{H}_{11}\text{N}_3\text{O}_4\text{S}$, 329.1, found 352.0 $[\text{M} + \text{Na}]^+$, 327.9 $[\text{M} - \text{H}]^-$. HPLC2: t_R 14.87 min, purity 98.8%.

2-(4-nitrophenyl)-4, 5-dihydro-1H-imidazole (7x)

Yield: 70.3 %. $^1\text{H NMR}$ (500MHz, CDCl_3) δ 8.30 (d, $J = 9.0$ Hz, 2 H), 7.98 (d, $J = 8.5$ Hz, 2 H), 3.88–3.95 (m, 4 H). MS (ESI): calculated for $\text{C}_9\text{H}_9\text{N}_3\text{O}_2$, 191.1, found 191.9 $[\text{M} + \text{H}]^+$, 189.7 $[\text{M} - \text{H}]^-$.

2-(4-Fluorophenyl)-4, 5-dihydro-1H-imidazole (7b)

Yield: 60.2 %. $^1\text{H NMR}$ (500MHz, CDCl_3) δ 7.80 (q, $J = 7.0$ Hz, 2 H), 7.11 (d, $J = 10.0$ Hz, 2 H), 3.82 (br, 4 H). MS (ESI): calculated for $\text{C}_9\text{H}_9\text{FN}_2$, 164.1, found 165 $[\text{M} + \text{H}]^+$.

2-(4-Methoxyphenyl)-4, 5-dihydro-1H-imidazole (7c)

Yield: 56.9%. ¹H NMR (500MHz, CDCl₃) δ 7.84 (d, *J* = 8.5 Hz, 2 H), 6.94 (d, *J* = 9.0 Hz, 2 H), 3.87 (s, 3 H), 3.85 (br, 4 H). MS (ESI): calculated for C₁₀H₁₂N₂O, 176.1, found 177.0 [M + H]⁺.

(4-Methoxyphenyl)(2-phenyl-1-(phenylsulfonyl)-1H-imidazol-4-yl)methanone (4ab)

Yield: 26.3%; mp 118 – 120 °C. ¹H NMR (500MHz, DMSO) δ 8.37 (d, *J* = 1.0 Hz, 1 H), 8.15–8.18 (m, 2 H), 8.12 (d, *J* = 9.0 Hz, 2 H), 7.56–7.64 (m, 5 H), 7.46–7.50 (m, 3 H), 7.16 (d, *J* = 8.0 Hz, 2 H), 3.90 (s, 3 H). MS (ESI): calculated for C₂₃H₁₈N₂O₄S, 418.1, found 419.1 [M + H]⁺. HPLC2: *t*_R 17.72 min, purity 95.7%.

(3-Methoxyphenyl)(2-phenyl-1-(phenylsulfonyl)-1H-imidazol-4-yl)methanone (4ac)

Yield: 31.2%; mp 136 – 138 °C. ¹H NMR (500MHz, CDCl₃) δ 8.35 (s, 1 H), 7.86 (d, *J* = 8.0 Hz, 1 H), 7.72 (s, 1 H), 7.60 (t, *J* = 7.5 Hz, 1 H), 7.51 (t, *J* = 7.5 Hz, 1 H), 7.35–7.42 (m, 9H), 7.14 (dd, *J* = 8.0 Hz, 2.0 Hz, 1 H), 3.88 (s, 3 H). MS (ESI): calculated for C₂₃H₁₈N₂O₄S, 418.1, found 419.1 [M + H]⁺. HPLC2: *t*_R 17.56 min, purity 97.4%.

(2-Phenyl-1-(phenylsulfonyl)-1H-imidazol-4-yl)(p-tolyl)methanone (4ah)

Yield: 28.9%; mp 108 – 110 °C. ¹H NMR (500MHz, CDCl₃) δ 8.00 (d, *J* = 7.5 Hz, 2 H), 7.98 (q, *J* = 8.0 Hz, 1.5 Hz, 2 H), 7.91 (d, *J* = 8.0 Hz, 1 H), 7.81 (s, 1 H), 7.44–7.48 (m, 3 H), 7.35–7.40 (m, 2 H), 7.30 (t, *J* = 8.0 Hz, 2 H), 7.20 (s, 2 H), 2.42 (s, 3 H). MS (ESI): calculated for C₂₃H₁₈N₂O₃S, 402.1, found 403.1 [M + H]⁺. HPLC2: *t*_R 16.06 min, purity 96.2%.

(4-Fluorophenyl)(2-phenyl-1-(phenylsulfonyl)-1H-imidazol-4-yl)methanone(4af)

Yield: 25.4%; mp 114 – 116 °C. ¹H NMR (500MHz, CDCl₃) δ 8.10 (q, *J* = 3.5 Hz, 5.5 Hz, 2 H), 7.88 (d, *J* = 7.5 Hz, 2 H), 7.67 (t, *J* = 7.5 Hz, 1 H), 7.48 – 7.54 (m, 3 H), 7.38 – 7.41 (m, 5 H), 7.24 (t, *J* = 8.5 Hz, 2 H). MS (ESI): calculated for C₂₂H₁₅FN₂O₃S, 406.1, found 429.1 [M + Na]⁺. HPLC2: *t*_R 15.43 min, purity 96.1%.

(3-Fluorophenyl)(2-phenyl-1-(phenylsulfonyl)-1H-imidazol-4-yl)methanone(4ag)

Yield: 18.3%; mp 102 – 104 °C. ¹H NMR (500MHz, CDCl₃) δ 8.14 (d, *J* = 7.5 Hz, 1 H), 7.76 – 7.87 (m, 3 H), 7.74 (d, *J* = 9.0 Hz, 1 H), 7.37 – 7.57 (m, 10 H), 7.38 – 7.41 (m, 5 H), 7.24 (t, *J* = 8.5 Hz, 2 H). MS (ESI): calculated for C₂₂H₁₅FN₂O₃S, 406.1, found 429.1 [M + Na]⁺. HPLC2: *t*_R 15.75 min, purity 96.5%.

(4-Fluorophenyl)(2-(4-methoxyphenyl)-1-(phenylsulfonyl)-1H-imidazol-4-yl) methanone (4cb)

Yield: 23.5%; mp 135 – 137 °C. ¹H NMR (500MHz, CDCl₃) δ 8.00 (d, *J* = 5.5 Hz, 2 H), 7.74 – 7.76 (m, 2 H), 7.54–7.58 (m, 1 H), 7.40 (d, *J* = 7.0 Hz, 2 H), 7.28–7.30 (m, 3H), 7.14 – 7.16 (m, 2 H), 6.80–6.82 (m, 2 H), 3.80 (s, 3 H). MS (ESI): calculated for C₂₃H₁₇FN₂O₄S, 436.1, found 459.0 [M + Na]⁺, 434.9 [M – H]⁻. HPLC2: *t*_R 16.53 min, Purity 96.1%.

(4-Fluorophenyl)(1-(phenylsulfonyl)-2-(p-tolyl)-1H-imidazol-4-yl) methanone (4db)

Yield: 18.6%; mp 142 – 144 °C. ¹H NMR (500MHz, CDCl₃) δ 8.07 (q, *J* = 8.5 Hz, 5.5 Hz, 2 H), 7.88 (d, *J* = 7.5 Hz, 2 H), 7.64 (t, *J* = 8.0 Hz, 1 H), 7.49 (d, *J* = 8.0 Hz, 2 H), 7.38 (s, 1H), 7.30 (d, *J* = 8.0 Hz, 2 H), 7.18 – 7.24 (m, 4 H), 2.43 (s, 3 H). MS (ESI): calculated for C₂₃H₁₇FN₂O₃S, 420.1, found 443.0 [M + Na]⁺, 418.9 [M – H]⁻. HPLC2: *t*_R 17.28 min, purity 97.3%.

(1-(Phenylsulfonyl)-2-(3, 4, 5-trimethoxyphenyl)-1H-imidazol-4-yl)(3, 4, 5-trimethoxyphenyl)methanone (4ea)

Yield: 21.1%; mp 135 – 137 °C. ¹H NMR (500MHz, CDCl₃) δ 7.91 (d, *J*=8.0 Hz, 2 H), 7.65 (t, *J*=7.5 Hz, 1 H), 7.51 (t, *J*=8.0 Hz, 2 H), 7.44 (s, 1 H), 7.34 (s, 2 H), 6.60 (s, 2 H), 3.98 (s, 3 H), 3.96 (s, 6 H), 3.91 (s, 3 H), 3.73 (s, 6 H). MS (ESI): calculated for C₂₈H₂₈N₂O₉S, 568.2, found 569.2 [M + H]⁺. HPLC1: *t*_R 17.86 min, purity 98.9%.

(4-fluorophenyl)(1-(phenylsulfonyl)-2-(3,4,5-trimethoxyphenyl)-1H-imidazol-4-yl)methanone (4eb)

Yield: 18.8%; mp 135 – 137 °C. ¹H NMR (500MHz, CDCl₃) δ 8.11 (q, *J*=5.5 Hz, 3.0 Hz, 1 H), 8.00 – 8.03 (m, 1 H), 7.82 (d, *J*=7.5 Hz, 1 H), 7.78 (s, 1 H), 7.64 (t, *J*=7.0 Hz, 1 H), 7.48 (t, *J*=8.0 Hz, 1 H), 7.42 (s, 1 H), 7.21 – 7.26 (m, 4 H), 6.62 (s, 1 H), 3.98 (s, 3 H), 3.96 (s, 6 H), 3.93 (s, 3 H). MS (ESI): calculated for C₂₅H₂₁FN₂O₆S, 496.1, found 497.1 [M + H]⁺. HPLC2: *t*_R 15.26 min, purity 98.5%.

(2-(4-Chlorophenyl)-1-(phenylsulfonyl)-1H-imidazol-4-yl)(4-fluorophenyl)methanone (4fb)

Yield: 36.8%; mp 153 – 155 °C. ¹H NMR (500MHz, CDCl₃) δ 8.06 (q, *J*=5.5 Hz, 3.0 Hz, 2 H), 7.89 (d, *J*=7.5 Hz, 2 H), 7.68 (t, *J*=8.0 Hz, 1 H), 7.52 (t, *J*=8.0 Hz, 2 H), 7.34–7.38 (m, 5H), 7.23 (t, *J*=8.5 Hz, 2 H). MS (ESI): calculated for C₂₂H₁₄ClFN₂O₃S, 440.0, found 463.0 [M + Na]⁺. HPLC2: *t*_R 17.72 min, purity 97.4%.

(2-(4-(Dimethylamino)phenyl)-1-(phenylsulfonyl)-1H-imidazol-4-yl)(3, 4, 5-trimethoxyphenyl)methanone (4ga)

Yield: 32.2%; mp 157 – 159 °C. ¹H NMR (500MHz, CDCl₃) δ 7.89 (d, *J*=8.0 Hz, 2 H), 7.62 (t, *J*=7.5 Hz, 1 H), 7.48 (t, *J*=8.0 Hz, 2 H), 7.43 (s, 1 H), 7.32 (d, *J*=8.5 Hz, 2 H), 7.30 (s, 2H), 6.62 (d, *J*=9.0 Hz, 2 H), 3.97 (s, 3 H), 3.95 (s, 6 H), 3.05 (s, 6 H). MS (ESI): calculated for C₂₇H₂₇N₃O₆S, 521.2, found 544.1 [M + Na]⁺, 519.8 [M – H][–]. HPLC2: *t*_R 16.00 min, purity 97.9%.

(2-(4-(Dimethylamino)phenyl)-1-(phenylsulfonyl)-1H-imidazol-4-yl)(4-fluorophenyl)methanone (4gb)

Yield: 38.5%; mp 125 – 127 °C. ¹H NMR (500MHz, CDCl₃) δ 8.04 (q, *J*=5.5 Hz, 3.5 Hz, 2 H), 7.80 (d, *J*=7.5 Hz, 2 H), 7.61 (t, *J*=8.0 Hz, 1 H), 7.45 (t, *J*=8.0 Hz, 2 H), 7.39 (s, 1 H), 7.35 (d, *J*=9.0 Hz, 2 H), 7.21 (t, *J*=8.5 Hz, 2 H), 6.62 (d, *J*=9.0 Hz, 2 H), 3.05 (s, 6 H). MS (ESI): calculated for C₂₄H₂₀FN₃O₃S, 449.1, found 472.1 [M + Na]⁺, 447.9 [M – H][–]. HPLC2: *t*_R 16.85 min, purity 96.5%.

(2-(3, 4-Dimethoxyphenyl)-1-(phenylsulfonyl)-1H-imidazol-4-yl)(3,4,5-trimethoxyphenyl)methanone (4ha)

Yield: 28.6%; mp 136 – 138 °C. ¹H NMR (300MHz, CDCl₃) δ 7.92 (dd, *J*=8.5 Hz, 1.5 Hz, 2 H), 7.66 (t, *J*=7.5 Hz, 2 H), 7.51 (t, *J*=7.5 Hz, 2 H), 7.43 (s, 1 H), 7.33 (s, 2 H), 7.02 (dd, *J*=8.0 Hz, 2.0 Hz, 1 H), 6.91 (d, *J*=2.0 Hz, 1 H), 6.86 (d, *J*=8.5 Hz, 1 H), 3.98 (s, 3 H), 3.96 (s, 9 H), 3.77 (s, 3 H). MS (ESI): calculated for C₂₇H₂₆N₂O₈S, 538.1, found 561.1 [M + Na]⁺, 536.8 [M – H][–]. HPLC2: *t*_R 14.67 min, purity 98.2%.

(2-(3, 4-Dimethoxyphenyl)-1-(phenylsulfonyl)-1H-imidazol-4-yl)(4-fluorophenyl)methanone (4hb)

Yield: 31.9%; mp 144 – 145 °C. ¹H NMR (300MHz, CDCl₃) δ 8.09 (q, *J*=5.5 Hz, 3.5 Hz, 2 H), 7.81 (d, *J*=8.0 Hz, 2 H), 7.62 (t, *J*=7.5 Hz, 2 H), 7.48 (t, *J*=7.5 Hz, 2 H), 7.40 (s, 1 H), 7.21–7.25 (m, 2 H), 7.04 (dd, *J*=8.0 Hz, 2.0 Hz, 1 H), 6.92 (d, *J*=2.0 Hz, 1 H), 6.86 (d, *J*

=8.5 Hz, 1 H), 3.96 (s, 3 H), 3.79 (s, 6 H). MS (ESI): calculated for $C_{24}H_{19}FN_2O_5S$, 466.1, found 489.1 $[M + Na]^+$, 464.8 $[M - H]^-$. HPLC2: t_R 15.52 min, purity 97.4%.

(1-(Phenylsulfonyl)-2-(2-(trifluoromethyl)phenyl)-1H-imidazol-4-yl)(3,4,5-trimethoxyphenyl) methanone (4ia)

Yield: 25.0%; mp 155 – 157 °C. 1H NMR (500MHz, DMSO) δ 7.91 (d, J =8.0 Hz, 1 H), 7.84 (q, J =7.5 Hz, 5.0 Hz, 2 H), 7.77–7.80 (m, 2 H), 7.75 (s, 2 H), 7.66 (t, J =8.0 Hz, 2 H), 7.56 (d, J =7.5 Hz, 1 H), 7.18 (s, 2 H), 3.87 (s, 6 H), 3.81 (s, 3 H). MS (ESI): calculated for $C_{26}H_{21}F_3N_2O_6S$, 546.1, found 569.0 $[M + Na]^+$. HPLC2: t_R 16.16 min, purity 98.9%.

(1-(Phenylsulfonyl)-2-(2-(trifluoromethyl)phenyl)-1H-imidazol-4-yl)(4-fluorophenyl) methanone (4ib)

Yield: 25.0%; mp 151 – 153 °C. 1H NMR (500MHz, $CDCl_3$) δ 8.03 (q, J =5.5 Hz, 3.0 Hz, 2 H), 7.90 (d, J =8.0 Hz, 2 H), 7.80 (d, J =8.0 Hz, 1 H), 7.69 (q, J =7.0 Hz, 6.5 Hz, 2 H), 7.61 (t, J =8.0 Hz, 1 H), 7.52 (t, J =8.0 Hz, 2 H), 7.34 – 7.36 (m, 2 H), 7.23 (t, J =8.5 Hz, 2 H). MS (ESI): calculated for $C_{23}H_{14}F_4N_2O_3S$, 474.1, found 497.0 $[M + Na]^+$. HPLC2: t_R 16.80 min, purity 98.2%.

(2-(4-(Benzyloxy)phenyl)-1-(phenylsulfonyl)-1H-imidazol-4-yl)(4-fluorophenyl) methanone (4jb)

Yield: 22.3.0%; mp 149 – 151 °C. 1H NMR (500MHz, $CDCl_3$) δ 8.09 (q, J =5.5 Hz, 3.5 Hz, 2 H), 7.82 (d, J =7.5 Hz, 2 H), 7.63 (t, 7.5 Hz, 1 H), 7.36–7.50(m, 10 H), 7.25 (t, J =8.5 Hz, 2 H), 6.98 (d, J =8.0 Hz, 2 H), 5.17 (s, 2 H). MS (ESI): calculated for $C_{29}H_{21}FN_2O_4S$, 512.1, found 535.0 $[M + Na]^+$. HPLC2: t_R 18.35 min, purity 95.1%.

(1-(Phenylsulfonyl)-2-(4-(trifluoromethyl)phenyl)-1H-imidazol-4-yl)(3,4,5-trimethoxyphenyl) methanone (4ia)

Yield: 36.7 %; 1H NMR ($CDCl_3$, 500MHz) δ 8.06 (d, J =7.5 Hz, 2 H), 7.78 (t, J =8.0 Hz, 1 H), 7.72 (d, J =8.0 Hz, 2 H), 7.62 (d, J =8.0 Hz, 2 H), 7.59 (d, J =8.0 Hz, 2 H), 7.50 (s, 1 H), 7.37 (s, 2 H), 4.04 (s, 3 H), 4.02 (s, 6 H). MS (ESI) calcd for $C_{26}H_{21}F_3N_2O_6S$ 546.1, found 547.1 $[M + H]^+$.

(2-Phenyl-1H-imidazol-4-yl)(3,4,5-trimethoxyphenyl)methanone (5aa)

Yield: 10.1 %; mp 227–229 °C. 1H NMR (500MHz, $CDCl_3$) δ 8.0–8.03 (m, 2 H), 7.83 (s, 1 H), 7.34–7.38 (m, 3 H), 7.21 (s, 2 H), 3.90 (s, 3 H), 3.84 (s, 6 H). MS (ESI): calculated for $C_{19}H_{18}N_2O$, 338.1, found 337.1 $[M - H]^-$. HPLC2: t_R 14.19 min, purity 96.3%.

(4-Methoxyphenyl)(2-phenyl-1H-imidazol-4-yl)methanone (5ab)

Yield: 16.6%; mp 179 – 181 °C. 1H NMR (500MHz, $CDCl_3$) δ 11.1 (br, 1 H), 8.07–8.10 (m, 2 H), 8.04 (d, J =8.5 Hz, 2 H), 7.84 (d, J =1.0 Hz, 1 H), 7.49–7.51 (m, 3 H), 7.07 (d, J =9.0 Hz, 2 H), 3.95 (s, 3 H). MS (ESI): calculated for $C_{17}H_{14}N_2O_2$, 278.1, found 279.0 $[M + H]^+$. HPLC1: t_R 15.14 min, purity > 99%.

(3-Methoxyphenyl)(2-phenyl-1H-imidazol-4-yl)methanone (5ac)

Yield: 22.5 %; mp 160 – 162 °C. 1H NMR (500MHz, $CDCl_3$) δ 11.2 (br, 1 H), 8.10–8.12 (m, 2 H), 7.87 (d, J =1.0 Hz, 1 H), 7.61 (d, J =7.5 Hz, 1 H), 7.48 – 7.52 (m, 5 H), 7.21 (dd, J =2.5 Hz, 8.5Hz, 1 H), 3.91 (s, 3 H). MS (ESI): calculated for $C_{17}H_{14}N_2O_2$, 278.1, found 279.0 $[M + H]^+$. HPLC2: t_R 15.07 min, purity > 99%.

(3, 5-Dimethoxyphenyl)(2-phenyl-1*H*-imidazol-4-yl)methanone (5ad)

Yield: 26.2%; mp 168 – 170 °C. ¹H NMR (500MHz, CDCl₃) δ 8.04–8.06 (m, 2 H), 7.88 (s, 1 H), 7.50–7.52 (m, 3 H), 7.15 (d, *J* = 2.0 Hz, 2 H), 6.75 (t, *J* = 1.0 Hz, 1 H), 3.89 (s, 6 H). MS (ESI): calculated for C₁₈H₁₆N₂O₃, 308.1, found 331.1 [M + Na]⁺, 306.9 [M – H][–]. HPLC2: *t*_R 15.59 min, purity > 99%.

(3, 4-Dimethoxyphenyl)(2-phenyl-1*H*-imidazol-4-yl)methanone (5ae)

Yield: 18.6%; mp 162 – 164 °C. ¹H NMR (500MHz, CDCl₃) δ 10.9 (br, 1 H), 8.05 (dd, *J* = 1.5 Hz, 8.0 Hz, 2 H), 7.86 (d, *J* = 1.5 Hz, 1 H), 7.74 (dd, *J* = 2.0 Hz, 8.5 Hz, 1 H), 7.56 (d, *J* = 2.0 Hz, 1 H), 7.50–7.52 (m, 3 H), 7.04 (d, *J* = 8.5 Hz, 1 H), 4.03 (s, 3 H), 3.99 (s, 3 H). MS (ESI): calculated for C₁₈H₁₆N₂O₃, 308.1, found 331.1 [M + Na]⁺, 306.9 [M – H][–]. HPLC2: *t*_R 13.54 min, purity > 99%.

(4-Fluorophenyl)(2-phenyl-1*H*-imidazol-4-yl)methanone (5af)

Yield: 30.2%; mp 231 – 233 °C. ¹H NMR (500MHz, CDCl₃) δ 10.6 (br, 1 H), 8.02–8.05 (m, 4 H), 7.81 (d, *J* = 1.0 Hz, 1 H), 7.51–7.54 (m, 3 H), 7.27 (t, *J* = 8.5 Hz, 2 H). MS (ESI): calculated for C₁₆H₁₁FN₂O, 266.1, found 267.0 [M + H]⁺, 264.8 [M – H][–]. HPLC1: *t*_R 15.37 min, purity 98.9%.

(3-Fluorophenyl)(2-phenyl-1*H*-imidazol-4-yl)methanone (5ag)

Yield: 23.4%; mp 212 – 214 °C. ¹H NMR (500MHz, CDCl₃) δ 8.05 (dd, *J* = 1.5 Hz, 7.5 Hz, 2 H), 7.86 (s, 1 H), 7.84 (d, *J* = 7.0 Hz, 1 H), 7.74 (d, *J* = 8.5 Hz, 1 H), 7.52–7.58 (m, 4 H), 7.37 (dt, *J* = 2.0 Hz, 6.0 Hz, 1 H). MS (ESI): calculated for C₁₆H₁₁FN₂O, 266.1, found 267.0 [M + H]⁺, 264.8 [M – H][–]. HPLC1: *t*_R 15.29 min, purity > 99%.

(2-Phenyl-1*H*-imidazol-4-yl)(*p*-tolyl)methanone (5ah)

Yield: 15.6%; mp 225 – 227 °C. ¹H NMR (500MHz, CDCl₃) δ 11.1 (br, 1 H), 8.08 (d, *J* = 7.5 Hz, 2 H), 7.93 (d, *J* = 9.0 Hz, 2 H), 7.84 (s, 1 H), 7.48–7.52 (m, 3 H), 7.38 (d, *J* = 10.0 Hz, 2 H), 2.50 (s, 3 H). MS (ESI): calculated for C₁₇H₁₄N₂O, 262.1, found 263.0 [M + H]⁺, 260.8 [M – H][–]. HPLC2: *t*_R 15.86 min, purity 98.7%.

(2-Phenyl-1*H*-imidazol-4-yl)(*m*-tolyl)methanone (5ai)

Yield: 20.5%; mp 168 – 169 °C. ¹H NMR (500MHz, CDCl₃) δ 11.0 (br, 1 H), 8.09–8.11 (m, 2 H), 7.84 (d, *J* = 1.5 Hz, 1 H), 7.81–7.82 (m, 2 H), 7.47–7.52 (m, 5 H), 2.50 (s, 3 H). MS (ESI): calculated for C₁₇H₁₄N₂O, 262.1, found 285.0 [M + Na]⁺, 260.8 [M – H][–]. HPLC2: *t*_R 15.89 min, purity > 99%.

(2-(4-Fluorophenyl)-1*H*-imidazol-4-yl)(3,4,5-trimethoxyphenyl) methanone (5ba)

Yield: 12.2%. mp 176 – 178 °C. ¹H NMR (500MHz, CDCl₃) δ 10.72 (br, 1 H), 8.02 (q, *J* = 5.0 Hz, 2 H), 7.84 (s, 1 H), 7.19 (t, *J* = 10.0 Hz, 2 H), 4.00 (s, 6 H), 3.97 (s, 3 H). MS (ESI): calculated for C₁₉H₁₇FN₂O₄, 356.1, found 379.1 [M + Na]⁺, 354.9 [M – H][–]. HPLC1: *t*_R 17.23 min, purity > 99%

(2-(4-Methoxyphenyl)-1*H*-imidazol-4-yl)(3,4,5-trimethoxyphenyl) methanone (5ca)

Yield: 10.2%; mp 220 – 222 °C. ¹H NMR (300MHz, CDCl₃) δ 10.24 (br, 1 H), 7.93 (d, *J* = 14.5 Hz, 2 H), 7.81 (s, 1 H), 7.24 (s, 2 H), 7.03 (d, *J* = 14.5 Hz, 2 H), 3.97 (s, 3 H), 3.95 (s, 6 H), 3.90 (s, 3 H). MS (ESI): calculated for C₂₀H₂₀N₂O₅, 368.1, found 391.0 [M + Na]⁺, 367.0 [M – H][–]. HPLC2: *t*_R 14.46 min, purity 98.4%.

(4-Fluorophenyl)(2-(4-methoxyphenyl)-1H-imidazol-4-yl)methanone (5cb)

Yield: 15.2%; mp 245 – 247 °C. ¹H NMR (500MHz, CDCl₃) δ 10.20 (br, 1 H), 7.93–7.96 (m, 2 H), 7.85 (d, *J* = 5.0 Hz, 2 H), 7.68 (s, 1 H), 7.15–7.17 (m, 2 H), 6.95 (d, *J* = 6.0 Hz, 2 H), 3.82 (s, 3 H). MS (ESI): calculated for C₁₇H₁₃FN₂O₂, 296.1, found 319.1 [M + Na]⁺, 294.9 [M – H][–]. HPLC2: *t*_R 15.40 min, purity 98.8%.

(2-(p-Tolyl)-1H-imidazol-4-yl)(3,4,5-trimethoxyphenyl)methanone (5da)

Yield: 48.5%; mp 201 – 203 °C. ¹H NMR (500MHz, CDCl₃) δ 10.40 (br, 1 H), 7.88 (d, *J* = 8.0 Hz, 2 H), 7.82 (s, 1 H), 7.31 (d, *J* = 8.0 Hz, 2 H), 7.24 (s, 2 H), 3.96 (s, 3 H), 3.94 (s, 6 H), 2.43 (s, 3 H). MS (ESI): calculated for C₂₀H₂₀N₂O₄, 352.1, found 375.2 [M + Na]⁺. HPLC2: *t*_R 15.45 min, purity 97.4%.

(4-Fluorophenyl)(2-(p-tolyl)-1H-imidazol-4-yl)methanone (5db)

Yield: 56.3%; mp 229 – 231 °C. ¹H NMR (500MHz, CDCl₃) δ 10.50 (br, 1 H), 7.99–8.02 (m, 2 H), 7.88 (d, *J* = 8.0 Hz, 2 H), 7.60 (d, *J* = 1.0 Hz, 1 H), 7.30 (d, *J* = 8.0 Hz, 2 H), 7.23 (t, *J* = 9.0 Hz, 2 H), 2.43 (s, 3 H). MS (ESI): calculated for C₁₇H₁₃FN₂O, 280.1, found 281.0 [M + H]⁺, 278.9 [M – H][–]. HPLC2: *t*_R 16.31 min, purity > 99%.

(3,4,5-Trimethoxyphenyl)(2-(3,4,5-trimethoxyphenyl)-1H-imidazol-4-yl)methanone (5ea)

Yield: 86.8%; mp 196 – 198 °C. ¹H NMR (500MHz, DMSO) δ 13.3 (br, 0.47 H), 13.50 (br, 0.52 H), 8.19 (s, 0.49 H), 7.90 (s, 1 H), 7.83 (s, 0.5 H), 7.59 (s, 1 H), 7.40 (s, 1 H), 7.18 (s, 1 H), 3.89 (s, 6 H), 3.86 (s, 6 H), 3.77 (s, 3 H), 3.72 (s, 3 H). MS (ESI): calculated for C₂₂H₂₄N₂O₇, 428.2, found 451.1[M + Na]⁺, 426.9 [M – H][–]. HPLC2: *t*_R 14.49 min, purity > 99%.

(4-Fluorophenyl)(2-(3,4,5-trimethoxyphenyl)-1H-imidazol-4-yl)methanone (5eb)

Yield: 90.2%; mp 153 – 155 °C. ¹H NMR (500MHz, CDCl₃) δ 10.42 (br, 1 H), 8.00 (q, *J* = 5.5 Hz, 3.0Hz, 2 H), 7.76 (s, 1H), 7.23 (t, *J* = 8.5 Hz, 2 H), 7.19 (s, 2 H), 3.94 (s, 3 H), 3.92 (s, 3 H). MS (ESI): calculated for C₁₉H₁₇FN₂O₄, 356.1, found 379.0 [M + Na]⁺, 354.9 [M – H][–]. HPLC2: *t*_R 15.31 min, purity > 99%.

(2-(4-Chlorophenyl)-1H-imidazol-4-yl)(3,4,5-trimethoxyphenyl)methanone (5fa)

Yield: 36.9%; mp 193 – 195 °C. ¹H NMR (500MHz, CDCl₃) δ 10.75 (br, 1 H), 7.96 (d, *J* = 8.5 Hz, 2 H), 7.83 (s, 1 H), 7.47 (d, *J* = 9.0 Hz, 2 H), 7.23 (s, 2 H), 3.97 (s, 3 H), 3.94 (s, 6 H), 2.43 (s, 3 H). MS (ESI): calculated for C₁₉H₁₇ClN₂O₄, 372.1, found 395.1 [M + Na]⁺, 370.9 [M – H][–]. HPLC2: *t*_R 16.36 min, purity > 99%.

(2-(4-Chlorophenyl)-1H-imidazol-4-yl)(4-fluorophenyl)methanone (5fb)

Yield: 83.7%; mp 232 – 234 °C. ¹H NMR (500MHz, CDCl₃) δ 10.78 (br, 1 H), 8.00 (q, *J* = 5.5 Hz, 3.0Hz, 2 H), 7.96 (d, *J* = 9.0 Hz, 2 H), 7.78 (s, 1 H), 7.47 (d, *J* = 8.0 Hz, 2 H), 7.24 (t, *J* = 8.5 Hz, 2 H). MS (ESI): calculated for C₁₆H₁₀ClFN₂O, 300.1, found 323.0 [M + Na]⁺, 298.8 [M – H][–]. HPLC2: *t*_R 17.08 min, purity > 99%.

(2-(4-(Dimethylamino)phenyl)-1H-imidazol-4-yl)(3,4,5-trimethoxyphenyl)methanone (5ga)

Yield: 91.2%; mp 195 – 197 °C. ¹H NMR (500MHz, CDCl₃) δ 10.39 (br, 1 H), 7.87 (d, *J* = 8.5 Hz, 2 H), 7.80 (s, 1 H), 7.23 (s, 2 H), 6.75(d, *J* = 9.0 Hz, 2 H), 3.95 (s, 3 H), 3.94 (s, 6 H), 3.05 (s, 6 H). MS (ESI): calculated for C₂₁H₂₃N₃O₄, 381.2, found 404.2 [M + Na]⁺, 380.0 [M – H][–]. HPLC2: *t*_R 15.20 min, purity 95.8%.

(2-(4-(Dimethylamino)phenyl)-1*H*-imidazol-4-yl)(4-fluorophenyl)methanone (5gb)

Yield: 86.7%; mp 278 – 280 °C. ¹H NMR (500MHz, CDCl₃) δ 10.21 (br, 1 H), 7.98 (q, *J* = 5.0 Hz, 3.5Hz, 2 H), 7.84 (d, *J* = 8.5 Hz, 2 H), 7.72 (s, 1 H), 7.20 (t, *J* = 8.5 Hz, 2 H), 6.76 (t, *J* = 9.0 Hz, 2 H), 3.06 (s, 6 H). MS (ESI): calculated for C₁₈H₁₆FN₃O, 309.1, found 332.1 [M + Na]⁺, 307.9 [M – H][–]. HPLC2: *t*_R 16.06 min, purity 95.6%.

(2-(3,4-Dimethoxyphenyl)-1*H*-imidazol-4-yl)(3,4,5-trimethoxyphenyl)methanone (5ha)

Yield: 85.0 %; mp 100 – 102 °C. ¹H NMR (500MHz, CDCl₃) δ 10.19 (br, 1 H), 7.81 (s, 1 H), 7.58 (d, *J* = 1.5 Hz, 1 H), 7.48 (d, *J* = 8.0 Hz, 1 H), 7.25 (s, 2 H), 6.97 (d, *J* = 8.5 Hz, 1 H), 4.00 (s, 3 H), 3.96 (s, 6 H), 3.95 (s, 6 H). MS (ESI): calculated for C₂₁H₂₂N₂O₆, 398.2, found 399.1 [M + H]⁺, 397.0 [M – H][–]. HPLC2: *t*_R 13.73 min, purity > 99%.

(2-(3,4-Dimethoxyphenyl)-1*H*-imidazol-4-yl)(4-fluorophenyl)methanone (5hb)

Yield: 78.3%; mp 174 – 176 °C. ¹H NMR (500MHz, CDCl₃) δ 8.02 (t, *J* = 9.0 Hz, 2 H), 7.75 (s, 1 H), 7.57 (s, 1 H), 7.48 (d, *J* = 8.5 Hz, 1 H), 7.23 (t, *J* = 8.5 Hz, 2 H), 6.95 (d, *J* = 8.5 Hz, 1 H), 3.99 (s, 3 H), 3.96 (s, 3 H). MS (ESI): calculated for C₁₈H₁₅FN₂O₃, 326.1, found 349.0 [M + Na]⁺, 324.9 [M – H][–]. HPLC2: *t*_R 14.65 min, purity > 99%.

(2-(2-(Trifluoromethyl)phenyl)-1*H*-imidazol-4-yl)(3,4,5-trimethoxyphenyl)methanone (5ia)

Yield: 83.8%; mp 75 – 77 °C. ¹H NMR (500MHz, CDCl₃) δ 10.37 (br, 1 H), 8.00–8.02 (m, 1 H), 7.87 (s, 1 H), 7.82–7.85 (m, 1 H), 7.69–7.74 (m, 1 H), 7.62–7.66 (m, 1 H), 7.25 (s, 2 H), 3.99 (s, 3 H), 3.98 (s, 6 H). MS (ESI): calculated for C₂₀H₁₇F₃N₂O₄, 406.1, found 429.1 [M + Na]⁺, 405.0 [M – H][–]. HPLC2: *t*_R 13.98 min, purity > 99%.

(4-Fluorophenyl)(2-(2-(trifluoromethyl)phenyl)-1*H*-imidazol-4-yl)methanone (5ib)

Yield: 91.1%; mp 152 – 154 °C. ¹H NMR (500MHz, CDCl₃) δ 8.12–8.14 (m, 2 H), 7.97 (d, *J* = 7.5 Hz, 1 H), 7.82–7.85 (m, 2 H), 7.69 (t, *J* = 7.5 Hz, 1 H), 7.61 (t, *J* = 8.0 Hz, 1 H), 7.22 (t, *J* = 9.0 Hz, 2 H). MS (ESI): calculated for C₁₇H₁₀F₄N₂O, 334.1, found 357.1 [M + Na]⁺, 332.9 [M – H][–]. HPLC2: *t*_R 15.10 min, purity > 99%.

(2-(4-(Benzyloxy)phenyl)-1*H*-imidazol-4-yl)(3,4,5-trimethoxyphenyl)methanone (5ja)

Yield: 16.5%; mp 191 – 193 °C. ¹H NMR (500MHz, CDCl₃) δ 10.22 (br, 1 H), 7.93 (d, *J* = 9.0 Hz, 2 H), 7.81 (s, 1 H), 7.37–7.47 (m, 5 H), 7.24 (s, 2 H), 7.11 (d, *J* = 8.5 Hz, 2 H), 5.16 (s, 2 H), 3.97 (s, 3 H), 3.95 (s, 6 H). MS (ESI): calculated for C₂₆H₂₄N₂O₅, 444.2, found 467.1 [M + Na]⁺, 442.9 [M – H][–]. HPLC2: *t*_R 17.36 min, purity 95.5%.

(2-(4-(Benzyloxy)phenyl)-1*H*-imidazol-4-yl)(4-fluorophenyl)methanone (5jb)

Yield: 84.7%; mp 212 – 214 °C. ¹H NMR (300MHz, CDCl₃) δ 10.28 (br, 1 H), 7.99–8.04 (m, 2 H), 7.92–7.95 (m, 2 H), 7.76 (d, *J* = 1.5 Hz, 1 H), 7.38–7.48 (m, 5 H), 7.20–7.25 (m, 2 H), 7.09–7.12 (m, 2 H), 5.16 (s, 2 H). MS (ESI): calculated for C₂₃H₁₇FN₂O₂, 372.1, found 395.1 [M + Na]⁺. HPLC2: *t*_R 17.97 min, purity 97.8%.

(2-(4-Hydroxyphenyl)-1*H*-imidazol-4-yl)(3,4,5-trimethoxyphenyl)methanone (5ka)

Yield: 72.3%. mp 191–193 °C. ¹H NMR (500MHz, CD₃OD) δ 8.31 (s, 1 H), 7.90 (d, *J* = 8.5 Hz, 2 H), 7.31 (s, 2 H), 7.05 (s, 2 H), 3.95 (s, 6 H), 3.88 (s, 3 H). MS (ESI): calculated for C₁₉H₁₈N₂O₅, 354.1, found 355.1 [M + H]⁺, 352.9 [M – H][–]. HPLC2: *t*_R 12.25 min, purity 98.7%.

(2-(4-(Hydroxyphenyl)-1*H*-imidazol-4-yl)(4-fluorophenyl)methanone (5kb)

Yield: 89.0%; mp 276 – 278 °C. ¹H NMR (500MHz, CDCl₃) δ 8.31 (s, 1 H), 8.13 (q, *J* = 5.5 Hz, 3.0 Hz, 2 H), 7.93 (d, *J* = 8.5 Hz, 2 H), 7.38 (t, *J* = 8.5 Hz, 2 H), 7.07 (d, *J* = 8.5 Hz, 2 H). MS (ESI): calculated for C₁₆H₁₁FN₂O₂, 282.1, found 283.0 [M + H]⁺, 280.9 [M – H][–]. HPLC2: *t*_R 13.46 min, purity 97.7%.

(2-(4-(Trifluoromethyl)phenyl)-1*H*-imidazol-4-yl)(3,4,5-trimethoxyphenyl)methanone (5la)

Yield: 85.3%; mp 195 – 196 °C. ¹H NMR (CDCl₃, 500MHz) δ 8.22 (d, *J* = 8.5 Hz, 2 H), 7.96 (s, 1 H), 7.83 (d, *J* = 8.5 Hz, 2 H), 7.34 (s, 2 H), 4.04 (s, 3 H), 4.00 (s, 6 H). MS (ESI) calcd for C₂₀H₁₇F₃N₂O₄ 406.1, found 407.1 [M + H]⁺. HPLC2: *t*_R 18.00 min, purity >99%.

(2-Phenyl-1*H*-imidazol-1-yl)(3,4,5-trimethoxyphenyl) methanone (5aaa)

Yield: 39.8%; mp 113 – 115 °C. ¹H NMR (500MHz, CDCl₃) δ 7.53 (q, *J* = 5.0 Hz, 3.0 Hz, 2 H), 7.41 (d, *J* = 1.0 Hz, 1 H), 7.33–7.35 (m, 3 H), 7.23 (d, *J* = 1.0 Hz, 1 H), 7.03 (s, 2 H), 3.93 (s, 3 H), 3.85 (s, 6 H). MS (ESI): calculated for C₁₉H₁₈N₂O₄, 338.1, found 339.1 [M + H]⁺. HPLC2: *t*_R 13.8 min, purity 95.6%.

(4-Methoxyphenyl)(2-phenyl-1*H*-imidazol-1-yl) methanone (5aba)

Yield: 56.3%; mp 68 – 70 °C. ¹H NMR (500MHz, CDCl₃) δ 7.78 (d, *J* = 9.0 Hz, 2 H), 7.54–7.56 (m, 2 H), 7.32–7.34 (m, 4 H), 7.21 (d, *J* = 1.0 Hz, 1 H), 6.93 (d, *J* = 8.5 Hz, 2 H), 3.90 (s, 3 H). MS (ESI): calculated for C₁₇H₁₄N₂O₂, 278.1, found 301.0 [M + Na]⁺, 276.8 [M – H][–]. HPLC2: *t*_R 14.72 min, purity 95.7%.

(4-Fluorophenyl)(2-(*p*-tolyl)-1*H*-imidazol-4-yl)methanone HCl salt (5db-HCl)

Yield: 95%; mp 115 – 117 °C. ¹H NMR (500MHz, DMSO) δ 8.20–8.23 (m, 2 H), 8.18 (s, 1 H), 8.04 (d, *J* = 6.5 Hz, 2 H), 7.42 (t, *J* = 8.0 Hz, 2 H), 7.37 (d, *J* = 7.0 Hz, 2 H), 2.38 (s, 3 H). MS (ESI): calculated for C₁₇H₁₄FCIN₂O, 316.1, found 281.0 [M – HCl + H]⁺. HPLC2: *t*_R 17.16 min, purity >99%.

(3,4,5-Trihydroxyphenyl)(2-(3,4,5-trihydroxyphenyl)-1*H*-imidazol-4-yl)methanone (6ea)

Yield: 66.1 %. mp 294 – 296 °C. ¹H NMR (500MHz, CD₃OD) δ 8.07 (s, 1 H), 7.07 (s, 2 H), 7.02 (s, 2 H). MS (ESI): calculated for C₁₆H₁₂N₂O₇, 344.1, found 345.0 [M + H]⁺, 342.9 [M – H][–]. HPLC2: *t*_R 3.62 min, purity 97.9%.

(2-(4-Chlorophenyl)-1*H*-imidazol-4-yl)(3,4,5-trihydroxyphenyl)methanone (6fa)

Yield: 79.3%; mp > 300 °C. ¹H NMR (500MHz, CD₃OD) δ 8.02 (d, *J* = 8.5 Hz, 2 H), 7.77 (s, 1 H), 7.54 (d, *J* = 8.5 Hz, 2 H), 7.14 (s, 2 H). MS (ESI): calculated for C₁₆H₁₁ClN₂O₄, 330.0, found 331.1 [M + Na]⁺, 328.9 [M – H][–]. HPLC2: *t*_R 11.9 min, purity 95.6%.

(2-(3,4-Dihydroxyphenyl)-1*H*-imidazol-4-yl)(3,4,5-trihydroxyphenyl)methanone (6ha)

Yield: 62.2 %; mp > 300 °C. ¹H NMR (500MHz, CD₃OD) δ 8.11 (s, 1 H), 7.46 (d, *J* = 2.0 Hz, 1 H), 7.42 (dd, *J* = 8.5 Hz, 2.0 Hz, 1 H), 7.10 (s, 2 H), 7.02 (d, *J* = 8.5 Hz, 1 H). MS (ESI): calculated for C₁₆H₁₂N₂O₆, 328.1, found 329.0 [M + H]⁺, 326.9 [M – H][–]. HPLC2: *t*_R 3.64 min, purity 97.9%.

Determination of aqueous solubility

The aqueous solubility of selected compounds was estimated using a miniaturized shake-flask method.³² Approximately 1 mg of each compound was suspended in either 1 mL water or pH 7.0 buffer in a glass vial and shaken at 450 rpm for 24 h at room temperature. The resulting mixture was centrifuged at 21,000 g for 10 min and the concentration in the

supernatant was measured by Acquity LC-MS/MS consisting of triple quadrupole mass spectrometer (Waters, Milford, MA) that was operated in positive ion mode with electrospray ionization. Chromatographic separation of the analytes was performed using a C6-phenyl column (50 mm × 2.1 i.d, 3.5 μM) (Phenomenex, Torrance, CA) with guard column, applying isocratic elution with water (10%) and acetonitrile (90%). The flow-rate was set to 0.5 ml/min.

Biology

Cell culture and cytotoxicity assay

We examined the antiproliferative activity of the ABI compounds in three melanoma cell lines (A375 and WM-164, human melanoma cell line; B16-F1, mouse melanoma cell line) and four human prostate cancer cell lines (LNCaP, DU 145, PC-3, and PPC-1). All these cell lines were purchased from ATCC (American Type Culture Collection, Manassas, VA) except the PPC-1 cell line which was kindly provided by Dr. Mitchell Steiner at the University of Tennessee Health Science Center. MDA-MB-435 and MDA-MB-435/LCCMDR1 cells were kindly provided by Dr. Robert Clarke at Georgetown University School of Medicine, Washington, DC. Melanoma cells were cultured in DMEM (Cellgro Mediatech, Inc., Herndon, VA) and prostate cancer cells were cultured in RPMI 1640 (Cellgro Mediatech, Inc., Herndon, VA) supplemented with 10% FBS (Cellgro Mediatech). Cultures were maintained at 37°C in a humidified atmosphere containing 5% CO₂. 1000 to 5000 cells were plated into each well of 96-well plates depending on growth rate and exposed to different concentrations of a test compound for 48 h (fast growing melanoma cells) or 96 h (slow growing prostate cancer cells) in three to five replicates. Cell numbers at the end of the drug treatment were measured by the sulforhodamine B (SRB) assay. Briefly, the cells were fixed with 10% trichloroacetic acid and stained with 0.4% SRB, and the absorbances at 540 nm were measured using a plate reader (DYNEX Technologies, Chantilly, VA). Percentages of cell survival versus drug concentrations were plotted, and the IC₅₀ (concentration that inhibited cell growth by 50% of untreated control) values were obtained by nonlinear regression analysis using GraphPad Prism (GraphPad Software, San Diego, CA).

Animals

Female C57/BL mice, age 4–6 weeks, were purchased from Harlan Laboratories (Harlan Laboratories Inc., Indianapolis, IN). Our animal housing met the Association for Assessment and Accreditation and Laboratory Animal Care specifications. All of the procedures were conducted in accordance with guidelines of our Institutional Animal Care and Use Committee.

In vivo evaluation of efficacy

Mouse melanoma B16-F1 cells were prepared in FBS-free DMEM medium (Cellgro Mediatech) at a concentration of 5×10^6 viable cells/mL. The cell suspension (100 μL) was injected subcutaneously in the right dorsal flank of each mouse. When tumor size reached about 100–150 mm³, about 7 days after cell inoculation, all mice bearing tumors were divided into control and treatment groups based on tumor size (n = 5 per group). Each group had similar average tumor size. Mice in control groups (negative control) were injected intraperitoneally with 50 μL vehicle solution only or DTIC at 60 mg/kg (positive control) once daily.²⁴ Tumor volume was measured every 2 days with a Traceable electronic digital caliper (Fisher Scientific, Inc., Pittsburgh, PA) and calculated using the formula $a \times b^2 \times 0.5$, where a and b represented the larger and smaller diameters, respectively.³³ Tumor volume was expressed in cubic millimeters. Data were expressed as mean ± SE for each group and

plotted as a function of time. Percentage tumor reduction at the conclusion of the experiment (14 days after starting treatment) was calculated with the formula $100 - 100 \times [(T - T_0)/(C - C_0)]$, where T represents mean tumor volume of a treated group on a specific day, T_0 represents mean tumor volume of the same group on the first day of treatment, C represents mean tumor volume of a control on a specific day, and C_0 represents mean tumor volume of the same group on the first day of treatment. Animal activity and average body weight of each group were monitored during the entire experiment period to assess compound toxicity. At the end of treatment, all mice were euthanized by CO_2 followed by cervical dislocation, and tumors were harvested for further studies.

In vitro microtubule polymerization assay

Bovine brain tubulin (0.4 mg) (Cytoskeleton, Denver, CO) was mixed with 10 μM of the test compound and incubated in 110 μl of general tubulin buffer (80 mM PIPES, 2.0 mM MgCl_2 , 0.5 mM EGTA, and 1 mM GTP) at pH 6.9. The absorbance at 340 nm was monitored every 1 min for 15 min by the SYNERGY 4 Microplate Reader (Bio-Tek Instruments, Winooski, VT). The spectrophotometer was set at 37 $^\circ\text{C}$ for tubulin polymerization.

Competitive colchicine binding assay

Each test compound was prepared at 20x concentration in G-PEM buffer (Cytoskeleton Inc., Denver, CO) followed by pipetting 10 μL of test compound into the 96-well plates. Ten microliters of tritiated labeled colchicine (Perkin-Elmer, Waltham, MA) was added to each testing well. Subsequently, 180 μL bead/tubulin (GE Healthcare Bio-Sciences Corp., Piscataway, NJ) suspension was added into each well. The plate was incubated for 45 min at 37 $^\circ\text{C}$ before it was read by a Topcount NXT plate reader (Perkin-Elmer, Waltham, MA). We included nonradiolabeled “cold” colchicine as a positive control and paclitaxel as a negative control because paclitaxel binds to a different site in tubulin and does not compete for the colchicine site binding. Data were processed using GraphPad Prism software.

Molecular modeling

All molecular modeling studies were performed with Schrodinger Molecular Modeling Suite 2009 (Schrodinger LLC, New York, NY), running on a Dell Linux workstation. Because the size of ABI compounds is much closer to that of ABT-751, rather than DAMA-colchicine, we selected tubulin complex with ABT-751 (PDB code: 3KHC) as our modeling system. ABIs were built and prepared using the Ligprep module, and they were docked into the ABT-751 site using the Glide module in Schrodinger Suite. The best docking complexes were subject to restricted molecular dynamics to release any strains using MacroModel module with OPLS-2005 forcefield. The ligand and its surrounding residues within 15 Å were allowed to move freely, while residues outside the 15 Å radius were kept rigid.

Supplementary Material

Refer to Web version on PubMed Central for supplementary material.

Acknowledgments

The project was supported by Grant Number 1R15CA125623-01A2 from NIH/NCI. Its contents are solely the responsibility of the authors and do not necessarily represent the official views of the NIH. Additional support comes from the Van Vleet Endowed Professorship (DDM), Division of Pharmaceutics, The Ohio State University, and GTx, Inc. Zhao Wang acknowledges the support from the Alma & Hal Reagan Fellowship. We thank Drs. Vivian S. Loveless and Christina Barrett for their help in the tubulin colchicine site binding assay and Dr. Ryan Yates for providing access to an HPLC instrument. We also thank Dr. David Armbruster, University of Tennessee Health Science Center library, for his editorial assistance.

Abbreviations

ABI	2-aryl-4-benzoyl-imidazole
AICA	2-aryl-imidazole-4-carboxylic amide
SMART	4-substituted methoxylbenzoyl-aryl-thiazole
MDR	multidrug resistant
IC₅₀	50 percent inhibition concentration
nM	nano-molar per liter
μM	micro-molar per liter
SPA	scintillation proximity assay
SAR	structure activity relationship
DTIC	dacarbazine
EDG	electron donating group
EWG	electron withdrawing group
Pgp	P-glycoprotein
DBU	1, 8-diazabicycloundec-7-ene
SRB	sulforhodamine B assay
DMSO	dimethyl sulfoxide
DMF	dimethylformamide
THF	tetrahydrofuran
TMS	tetramethylsilane
NMR	nuclear magnetic resonance
SEM	standard error of the mean
rt	room temperature
RP-HPLC	reverse phase-high performance liquid chromatography
ESI	electrospray ionization
LC-MS	liquid chromatography-mass spectrometry
PDB	protein data bank
TLC	thin layer chromatography

References

1. Chen J, Wang Z, Lu Y, Dalton JT, Miller DD, Li W. Synthesis and antiproliferative activity of imidazole and imidazoline analogs for melanoma. *Bioorg Med Chem Lett*. 2008; 18:3183–3187. [PubMed: 18477505]
2. Lu Y, Li CM, Wang Z, Ross CR 2nd, Chen J, Dalton JT, Li W, Miller DD. Discovery of 4-substituted methoxybenzoyl-aryl-thiazole as novel anticancer agents: synthesis, biological evaluation, and structure-activity relationships. *J Med Chem*. 2009; 52:1701–1711. [PubMed: 19243174]
3. Li F, Lu Y, Li W, Miller DD, Mahato RI. Synthesis, formulation and in vitro evaluation of a novel microtubule destabilizer, SMART-100. *Journal of Controlled Release*. 2010; 143:151–158. [PubMed: 20060430]

4. Amir E, Rozen S. Easy access to the family of thiazole N-oxides using HOF x CH₃CN. *Chem Commun (Camb)*. 2006;2262–2264. [PubMed: 16718323]
5. Williams, DA.; Lemke, TL. *Foye's Principles of Medicinal Chemistry*. 5. Lippincott Williams & Wilkins; Philadelphia: 2002.
6. Warburg O. On the origin of cancer cells. *Science*. 1956; 123:309–314. [PubMed: 13298683]
7. Ishihara M, Togo H. An Efficient Preparation of 2-Imidazolines and Imidazoles from Aldehydes with Molecular Iodine and (Diacetoxyiodo)benzene. *Synlett*. 2006; 2:227–230.
8. Williams DR, Lowder PD, Gu YG, Brooks DA. Studies of Mild Dehydrogenations in Heterocyclic System. *Tetrahedron Letters*. 1997; 38:331–334.
9. Haneda S, Okui A, Ueba C, Hayashi M. An efficient synthesis of 2-arylimidazoles by oxidation of 2-arylimidazolines using activated carbon–O₂ system and its application to palladium-catalyzed Mizoroki–Heck reaction. *Tetrahedron*. 2007; 63:2414–2417.
10. Amemiya Y, Miller DD, Hsu FL. Dehydrogenation of imidazolines to imidazoles with Pd-Carbon. *Synthetic Communications*. 1990; 20:2483–2489.
11. Jones H, Fordice MW, Greenwald RB, Hannah J, Jacobs A, Ruyle WV, Walford GL, Shen TY. Synthesis and analgesic-antiinflammatory activity of some 4- and 5-substituted heteroarylsalicylic acids. *J Med Chem*. 1977; 21:1100–1104. [PubMed: 309948]
12. Nakamura T, Sato M, Kakinuma H, Miyata N, Taniguchi K, Bando K, Koda A, Kameo K. Pyrazole and isoxazole derivatives as new, potent, and selective 20-hydroxy-5,8,11,14-eicosatetraenoic acid synthase inhibitors. *J Med Chem*. 2003; 46:5416–5427. [PubMed: 14640550]
13. Mahboobi S, Sellmer A, Burgemeister T, Lyssenko A, Schollmeyer D. Synthesis of Naturally Occurring Pyrazine and Imidazole Alkaloids from *Botryllus Leachi*. *Monatshfte fur Chemie*. 2004:333–342.
14. Lee JP, Lee SS. Kinetics and Mechanism for Hydrolysis Reaction of N-Benzoyl-2-phenylimidazole. *Bull Korean Chem Soc*. 2002; 23:151–153.
15. Bellina F, Cauteruccio S, Monti S, Rossi R. Novel imidazole-based combretastatin A-4 analogues: Evaluation of their in vitro antitumor activity and molecular modeling study of their binding to the colchicine site of tubulin. *Bioorganic & Medicinal Chemistry Letters*. 2006; 16:5757–5762. [PubMed: 16950621]
16. Wang L, Woods KW, Li Q, Barr KJ, McCroskey RW, Hannick SM, Gherke L, Credo RB, Hui YH, Marsh K, Warner R, Lee JY, Zielinski-Mozng N, Frost D, Rosenberg SH, Sham HL. Potent, Orally Active Heterocycle-Based Combretastatin A-4 Analogues: Synthesis, Structure Activity Relationship, Pharmacokinetics, and In Vivo Antitumor Activity Evaluation. *J Med Chem*. 2002; 45:1697–1711. [PubMed: 11931625]
17. Ross DT, Scherf U, Eisen MB, Perou CM, Rees C, Spellman P, Iyer V, Jeffrey SS, Van de Rijn M, Waltham M, Pergamenschikov A, Lee JC, Lashkari D, Shalon D, Myers TG, Weinstein JN, Botstein D, Brown PO. Systematic variation in gene expression patterns in human cancer cell lines. *Nat Genet*. 2000; 24:227–235. [PubMed: 10700174]
18. Sellappan S, Grijalva R, Zhou X, Yang W, Eli MB, Mills GB, Yu D. Lineage infidelity of MDA-MB-435 cells: expression of melanocyte proteins in a breast cancer cell line. *Cancer Res*. 2004; 64:3479–3485. [PubMed: 15150101]
19. Rae JM, Creighton CJ, Meck JM, Haddad BR, Johnson MD. MDA-MB-435 cells are derived from M14 melanoma cells--a loss for breast cancer, but a boon for melanoma research. *Breast Cancer Res Treat*. 2007; 104:13–19. [PubMed: 17004106]
20. Dong X, Mattingly CA, Tseng MT, Cho MJ, Liu Y, Adams VR, Mumper RJ. Doxorubicin and paclitaxel-loaded lipid-based nanoparticles overcome multidrug resistance by inhibiting P-glycoprotein and depleting ATP. *Cancer Res*. 2009; 69:3918–3926. [PubMed: 19383919]
21. Leonessa F, Green D, Licht T, Wright A, Wingate-Legette K, Lippman J, Gottesman MM, Clarke R. MDA435/LCC6 and MDA435/LCC6MDR1: ascites models of human breast cancer. *Br J Cancer*. 1996; 73:154–161. [PubMed: 8546900]
22. Zhang S, Morris ME. Effects of the flavonoids biochanin A, morin, phloretin, and silymarin on P-glycoprotein-mediated transport. *J Pharmacol Exp Ther*. 2003; 304:1258–1267. [PubMed: 12604704]

23. Vredenburg MR, Ojima I, Veith J, Pera P, Kee K, Cabral F, Sharma A, Kanter P, Greco WR, Bernacki RJ. Effects of orally active taxanes on P-glycoprotein modulation and colon and breast carcinoma drug resistance. *J Natl Cancer Inst.* 2001; 93:1234–1245. [PubMed: 11504769]
24. Povlsen CO, Jacobsen GK. Chemotherapy of a human malignant melanoma transplanted in the nude mouse. *Cancer Res.* 1975; 35:2790–2796. [PubMed: 1157050]
25. Li C-M, Lu Y, Narayanan R, Miller DD, Dalton JT. Drug metabolism and pharmacokinetics of 4-Substituted Methoxybenzoyl-Aryl-Thiazoles (SMART). *Drug Metab Dispos.* 2010 in press. 10.1124/dmd.110.034348
26. Lowe J, Li H, Downing KH, Nogales E. Refined structure of alpha beta-tubulin at 3.5 Å resolution. *J Mol Biol.* 2001; 313:1045–1057. [PubMed: 11700061]
27. Gigant B, Wang C, Ravelli RB, Roussi F, Steinmetz MO, Curmi PA, Sobel A, Knossow M. Structural basis for the regulation of tubulin by vinblastine. *Nature.* 2005; 435:519–522. [PubMed: 15917812]
28. Ravelli RB, Gigant B, Curmi PA, Jourdain I, Lachkar S, Sobel A, Knossow M. Insight into tubulin regulation from a complex with colchicine and a stathmin-like domain. *Nature.* 2004; 428:198–202. [PubMed: 15014504]
29. Tahir SK, Kovar P, Rosenberg SH, Ng SC. Rapid colchicine competition-binding scintillation proximity assay using biotin-labeled tubulin. *Biotechniques.* 2000; 29:156–160. [PubMed: 10907090]
30. Dorleans A, Gigant B, Ravelli RB, Mailliet P, Mikol V, Knossow M. Variations in the colchicine-binding domain provide insight into the structural switch of tubulin. *Proc Natl Acad Sci U S A.* 2009; 106:13775–13779. [PubMed: 19666559]
31. Rustin GJ, Shreeves G, Nathan PD, Gaya A, Ganesan TS, Wang D, Boxall J, Poupard L, Chaplin DJ, Stratford MR, Balkissoon J, Zweifel M. A Phase Ib trial of CA4P (combretastatin A-4 phosphate), carboplatin, and paclitaxel in patients with advanced cancer. *Br J Cancer.* 2010; 102:1355–1360. [PubMed: 20389300]
32. Glomme A, Marz J, Dressman JB. Comparison of a miniaturized shake-flask solubility method with automated potentiometric acid/base titrations and calculated solubilities. *J Pharm Sci.* 2005; 94:1–16. [PubMed: 15761925]
33. Guo W, Wu S, Liu J, Fang B. Identification of a small molecule with synthetic lethality for K-ras and protein kinase C iota. *Cancer Res.* 2008; 68:7403–7408. [PubMed: 18794128]

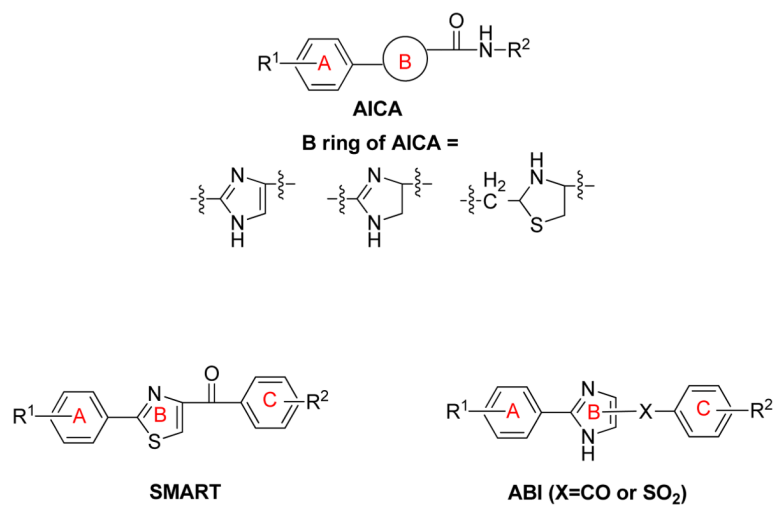


Figure 1.
General structures of AICA, SMART and ABI

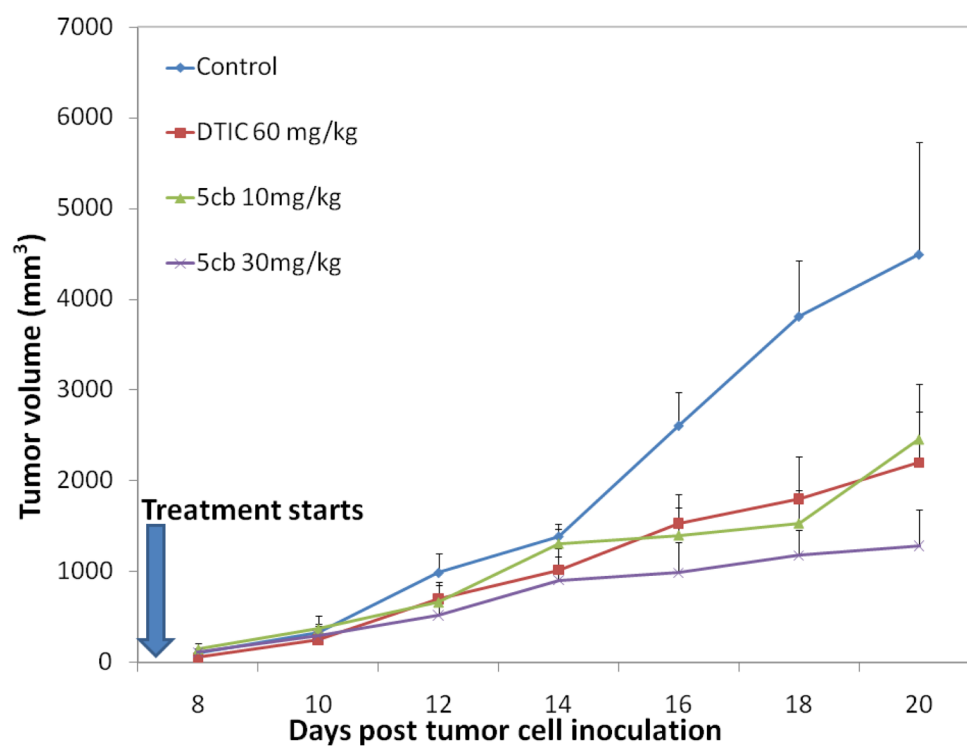


Figure 2.
In vivo study of **5cb** against B16-F1 melanoma tumors in C57/BL mice

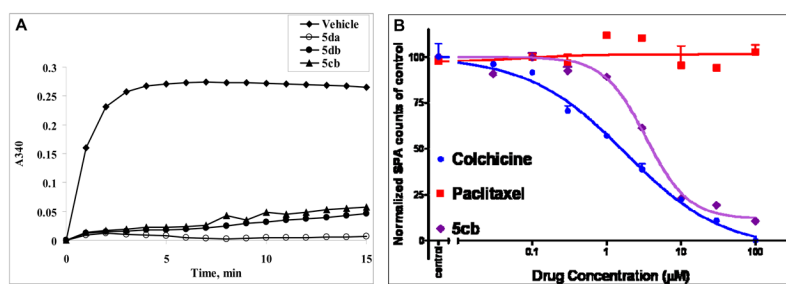


Figure 3.

A. Effect of ABI compounds on tubulin polymerization *in vitro*. Tubulin (0.4 mg/assay) was exposed to 10 μ M ABI compounds (vehicle control, 5% DMSO). Absorbance at 340 nm was monitored at 37°C every minute for 15 min; **B.** [3 H]-colchicine competition-binding scintillation proximity assay showed that ABI compounds competitively bound to tubulin colchicine binding site.

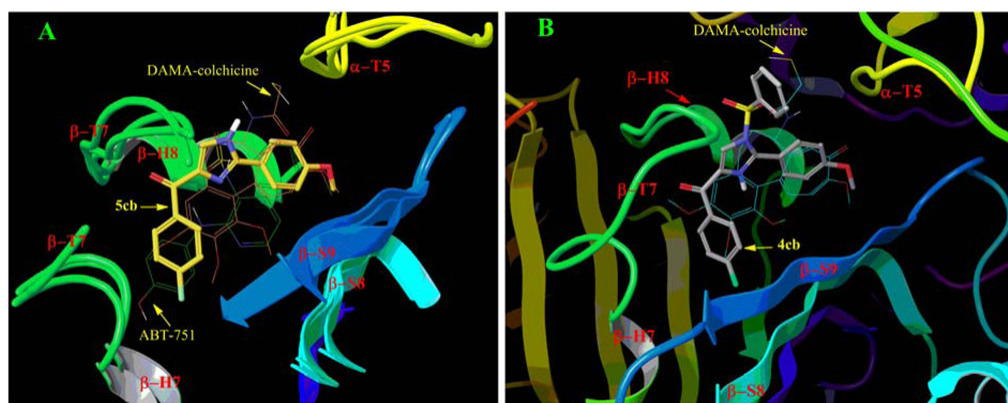
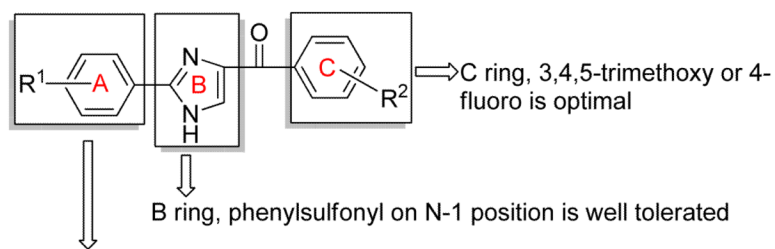
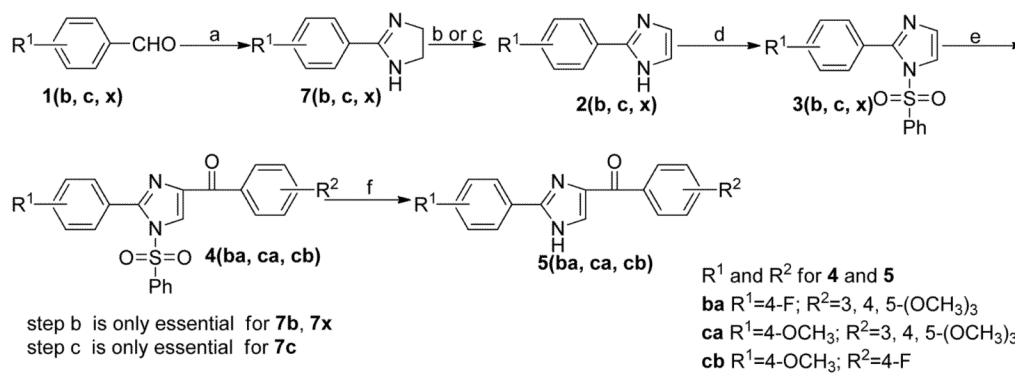


Figure 4.
Proposed binding mode of ABI analogs in the colchicine binding site.

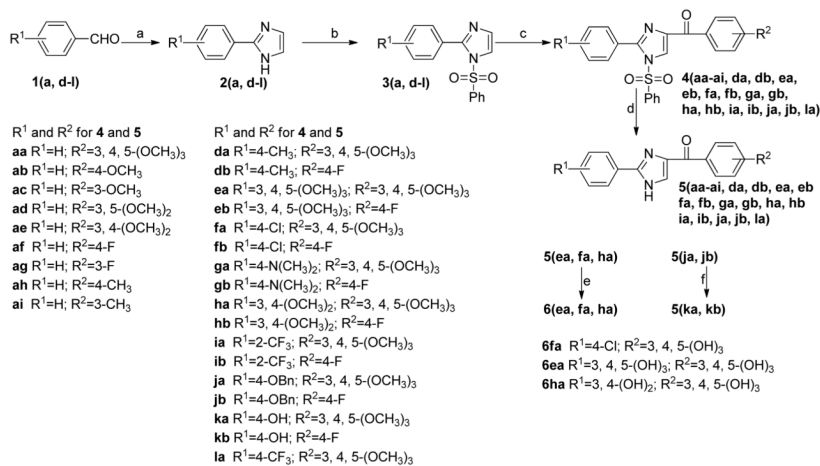


A ring, para substitution is the best. No specific requirement for the substituents, both electro-donating and withdrawing groups can improve activity compared with non-substituted A ring. Bulky group such as 3,4,5-trimethoxy abolishes activity

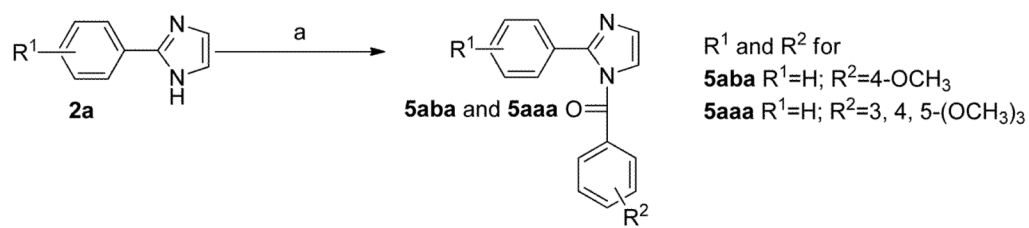
Figure 5.
SAR relationship of the ABI analogs

**Scheme 1.**

Reagents and conditions: (a) t-BuOH, I₂, Ethylenediamine, K₂CO₃, reflux; (b) PhI (OAc)₂, K₂CO₃, DMSO; (c) DBU, CBrCl₃, DMF; (d) NaH, PhSO₂Cl, THF, 0°C – rt; (e) t-BuLi, substituted benzoyl chloride, THF, –78°C; (f) Bu₄NF, THF, rt;

**Scheme 2.**

Reagents and conditions: (a) NH₄OH, oxalaldehyde, Ethanol, rt; (b) NaH, PhSO₂Cl, THF, 0°C – rt; (c) t-BuLi, substituted benzoyl chloride, THF, –78°C; (d) Bu₄NF, THF, rt; (e) BBr₃, CH₂Cl₂; (f) c-HCl, AcOH, reflux;

**Scheme 3.**

Reagents and conditions: (a) NaH, substituted benzoyl chloride, THF.

Table 1

In vitro growth inhibitory effects of compounds without A ring substitutions.

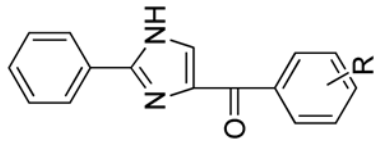
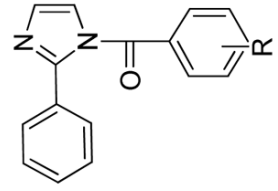
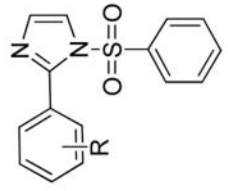
Structure	ID	R	IC ₅₀ ± SEM (μM)									
			A375	BI6-F1	WM164	LNCaP	PC-3	Du 145	PPC-1			
	5aa	3,4,5-(OMe) ₃	0.16±0.02	0.12±0.01	0.10±0.01	0.15±0.02	0.29±0.04	0.20±0.03	0.13±0.01	>10	>10	
	5ab	4-OMe	>10	>10	>10	>10	>10	>10	>10	>10	>10	
	5ac	3-OMe	>10	>10	>10	>10	>10	>10	>10	>10	>10	
	5ad	3, 5-(OMe) ₂	2.8±0.5	5.4±0.8	2.1±0.4	3.6±0.3	3.2±0.5	2.6±0.3	2.1±0.2	>10	>10	
	5ae	3, 4-(OMe) ₂	>10	>10	>10	>10	>10	>10	>10	>10	>10	
	5af	4-F	0.58±0.07	0.93±0.1	0.63±0.09	0.61±0.08	2.1±0.3	0.85±0.1	0.57±0.1	>10	>10	
	5ag	3-F	>10	>10	>10	>10	>10	>10	>10	>10	>10	
	5ah	4-Me	>10	>10	>10	>10	>10	>10	>10	>10	>10	
	5ai	3-Me	>10	>10	>10	>10	>10	>10	>10	>10	>10	
	5aba	4-OMe	>10	>10	>10	>10	>10	>10	>10	>10	>10	
5aaa	3,4,5-(OMe) ₃	>10	>10	>10	>10	>10	>10	>10	>10	>10		
	3a	H	>10	>10	>10	>10	>10	>10	>10	>10	>10	
	3x	4-NO ₂	>10	>10	>10	>10	>10	>10	>10	>10	>10	
	3j	4-OBn	>10	>10	>10	>10	>10	>10	>10	>10	>10	
			>10	>10	>10	>10	>10	>10	>10	>10	>10	

Table 2

In vitro growth inhibitory effects of compounds with substitutions on A ring

Structure	ID	R ¹	R ²	IC ₅₀ ± SEM (nM)							
				A375	BI6-F1	WM164	LNCaP	PC-3	Du 145	PPC-1	
	5ba	4-F	3,4,5-(OMe) ₃	205±19	320±41	73±8	98±2	169±12	132±24	81±1	
	5ca	4-OMe	3,4,5-(OMe) ₃	30±5	108±12	31±4	31±1	45±1	48±0.5	34±0.3	
	5cb	4-OMe	4-F	31±5	63±7	28±3	28±2	31±2	41±38	29±1	
	5da	4-Me	3,4,5-(OMe) ₃	9±2	46±5	8±2	12±1	9±0.4	15±0.5	11±0.1	
	5db	4-Me	4-F	142±13	222±10	156±19	45±2	65±3	78±5	54±1	
	5db-HCl			108±11	297±23	112±9	ND	ND	ND	ND	
	5ea	3,4,5-(OMe) ₃	3,4,5-(OMe) ₃	4800	>10000	>10000	>10000	>10000	>10000	>10000	
	5eb	3,4,5-(OMe) ₃	4-F	>10000	>10000	>10000	>10000	>10000	>10000	>10000	
	5fa	4-Cl	3,4,5-(OMe) ₃	43±5	168±14	26±3	24±1	35±1	36±0.4	26±0.2	
	5fb	4-Cl	4-F	52±4	73±6	74±9	49±2	81±2	65±1	52±1	
	6fa	4-Cl	3,4,5-(OH) ₃	3900	1810	2100	10000	10000	10000	>10000	
	5ga	4-N(Me) ₂	3,4,5-(OMe) ₃	82±9	361±29	80±11	58±2	92±4	95±1	67±0.7	
	5gb	4-N(Me) ₂	4-F	56±7	129±11	62±8	57±6	81±3	72±0.4	45±0.3	
	5ha	3,4-(OMe) ₂	3,4,5-(OMe) ₃	113±14	1400±200	191±18	121±10	203±7	168±15	117±1	
	5hb	3,4-(OMe) ₂	4-F	10000	4210	1400	2533	10000	10000	2172±48	
	5ia	2-CF ₃	3,4,5-(OMe) ₃	>10000	>10000	>10000	>10000	>10000	>10000	>10000	
	5ib	2-CF ₃	4-F	>10000	>10000	>10000	>10000	>10000	>10000	>10000	
	6ea	3,4,5-(OH) ₃	3,4,5-(OH) ₃	>10000	>10000	>10000	>10000	>10000	>10000	>10000	
	5ja	4-OBn	3,4,5-(OMe) ₃	5200	10000	5500	2786	10000	10000	2844	
	5jb	4-OBn	4-F	93±8	117±16	90±12	44±7	79±0.4	60±3	43±0.2	
	5ka	4-OH	3,4,5-(OMe) ₃	1600	2400	1800	ND	ND	ND	ND	
	5kb	4-OH	4-F	10000	>10000	>10000	10000	>10000	>10000	>10000	
	5la	4-CF ₃	3,4,5-(OMe) ₃	163±10	468±25	175±16	134±6	127±7	174±31	110±3	
	6ha	3,4-(OH) ₂	3,4,5-(OH) ₃	>10000	>10000	>10000	>10000	>10000	>10000	>10000	
	Colchicine			20±3	29±5	ND	16±4	11±1	10±2	20±1	

ND- not determined

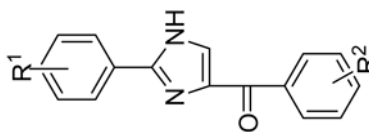


Table 3

In vitro growth inhibitory effects of compounds with protection on B ring

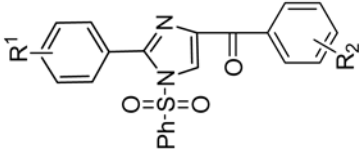
Structure	ID	R ¹	R ²	IC ₅₀ ± SEM (nM)									
				A375	B16-F1	WMI64	LNCaP	PC-3	Du 145	PPC-1			
	4ab	H	4-OMe	>10000	>10000	>10000	>10000	>10000	>10000	>10000	>10000	>10000	>10000
	4ac	H	3-OMe	>10000	>10000	>10000	>10000	>10000	>10000	>10000	>10000	>10000	>10000
	4ah	H	4-Me	>10000	>10000	>10000	>10000	>10000	>10000	>10000	>10000	>10000	>10000
	4af	H	4-F	630±72	946±86	596±61	573	2233	846	575			
	4ag	H	3-F	>10000	>10000	>10000	>10000	>10000	>10000	>10000	>10000	>10000	>10000
	4cb	4-OMe	4-F	36±5	71±8	43±6	31±2	33±2	52±3	32±0.7			
	4db	4-Me	4-F	113±14	287±31	107±14	55±3	80±1	80±1	57±1			
	4ea	3,4,5-(OMe) ₃	3,4,5-(OMe) ₃	>10000	>10000	>10000	>10000	>10000	>10000	>10000	>10000	>10000	>10000
	4eb	3,4,5-(OMe) ₃	4-F	3840	>10000	>10000	>10000	>10000	>10000	>10000	>10000	>10000	>10000
	4fb	4-Cl	4-F	88±9	107±12	70±6	48±1	76±2	64±1	54±1			
	4ga	4-N(Me) ₂	3,4,5-(OMe) ₃	162±13	1200±90	308±32	62±2	93±6	99±2	72±0.4			
	4gb	4-N(Me) ₂	4-F	55±7	242±26	56±4	56±6	83±3	74±0.5	48±0.3			
	4ha	3,4-(OMe) ₂	3,4,5-(OMe) ₃	192±15	970±68	139±15	114±6	197±9	144±29	117±2			
	4hb	3,4-(OMe) ₂	4-F	960±59	2000±400	1400±30	1915±77	10000	3312	1441±49			
4ia	2-CF ₃	3,4,5-(OMe) ₃	>10000	>10000	>10000	>10000	>10000	>10000	>10000	>10000	>10000	>10000	
4ib	2-CF ₃	4-F	>10000	>10000	>10000	>10000	>10000	>10000	>10000	>10000	>10000	>10000	
4jb	4-OBn	4-F	64±7	110±15	48±5	35±1	75±0.5	58±1	38±0.2				

Table 4

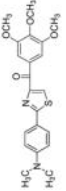
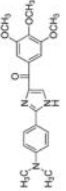
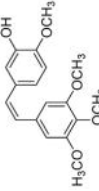
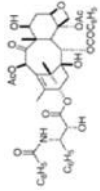
In vitro growth inhibitory effects of the ABI compounds in comparison to other anticancer drugs on multidrug-resistant melanoma cell line (MDR cell) and the matching sensitive parent cell line (Normal Melanoma cell).

Compound ID	IC ₅₀ ± SEM (nM) (n=3)		
	MDA-MB-435	MDA-MB-435/LCC6MDR1	Resistance index*
5cb	24±2	30±4	1.3
4cb	38±3	30±2	0.8
4fb	50±6	35±3	0.7
Paclitaxel	4±1	277±41	69.3
Vinblastine	0.4±0.1	11±1	27.5
Colchicine	10±1	658±50	65.8

* Resistance indexes were calculated by dividing IC₅₀ values on multidrug-resistant cell line MDA-MB-435/LCC6MDR1 by IC₅₀ values on the matching sensitive parental cell line MDA-MB-435.

Table 5

Aqueous solubility of ABI compound and its SMART counterpart as well as CA-4 and paclitaxel

Compound name	Structure	Media	Solubility (µg/mL)	Std Dev	%CV
SMART-1		Buffer pH 7.0	0.909	0.057	6.2
		Water	0.833	0.169	20.3
ABI-5ga		Buffer pH 7.0	48.9	5.59	11.4
		Water	11.3	1.70	15.0
Combretastatin A4		Buffer pH 7.0	1.04	0.147	14.2
		Water	2.83	0.330	11.7
Paclitaxel		Buffer pH 7.0	0.137	0.024	17.5
		Water	0.021	0.004	20.7